

## SOLAR SYSTEM ABUNDANCES AND CONDENSATION TEMPERATURES OF THE ELEMENTS

KATHARINA LODDERS

Planetary Chemistry Laboratory, Department of Earth and Planetary Sciences and McDonnell Center for the Space Sciences,  
Washington University, Campus Box 1169, St. Louis, MO 63130-4899; lodders@levee.wustl.edu.

Received 2003 January 22; accepted 2003 March 21

### ABSTRACT

Solar photospheric and meteoritic CI chondrite abundance determinations for all elements are summarized and the best currently available photospheric abundances are selected. The meteoritic and solar abundances of a few elements (e.g., noble gases, beryllium, boron, phosphorous, sulfur) are discussed in detail. The photospheric abundances give mass fractions of hydrogen ( $X = 0.7491$ ), helium ( $Y = 0.2377$ ), and heavy elements ( $Z = 0.0133$ ), leading to  $Z/X = 0.0177$ , which is lower than the widely used  $Z/X = 0.0245$  from previous compilations. Recent results from standard solar models considering helium and heavy-element settling imply that photospheric abundances and mass fractions are not equal to protosolar abundances (representative of solar system abundances). Protosolar elemental and isotopic abundances are derived from photospheric abundances by considering settling effects. Derived protosolar mass fractions are  $X_0 = 0.7110$ ,  $Y_0 = 0.2741$ , and  $Z_0 = 0.0149$ . The solar system and photospheric abundance tables are used to compute self-consistent sets of condensation temperatures for all elements.

*Subject headings:* astrochemistry — meteors, meteoroids — solar system: formation —  
Sun: abundances — Sun: photosphere

### 1. INTRODUCTION

The condensation temperatures of the elements from a solar composition gas are widely used as a diagnostic of chemical fractionation processes in astronomy, planetary science, and meteoritics. Wildt (1933) and Russell (1934) did probably the earliest thermochemical computations for gas chemistry in the Sun and for cool stars that also took condensation into account. Lord (1965) picked up on this theme, and since then, many studies have been dedicated to finding the volatility trends of the elements, which are expressed by the condensation temperature of an element and its compounds. Important studies include Larimer (1967, 1973), Grossman (1972), Grossman & Larimer (1974), Boynton (1975), Wai & Wasson (1977, 1979), Sears (1978), Fegley & Lewis (1980), Saxena & Eriksson (1983), Fegley & Palme (1985), Kornacki & Fegley (1986), and Palme & Fegley (1990). More recent studies have become quite detailed in investigating the condensation of major rock-forming elements under various potential nebular conditions, such as different dust-to-gas ratios (see, e.g., Ebel & Grossman 2000 and references therein).

Still, the available condensation temperatures, which have been calculated for almost all naturally occurring elements, are a melange from several studies dating back to the 1970s and 1980s (see summary tables in Wasson 1985 or Lodders & Fegley 1998). In addition, these condensation temperatures are a mixture of “condensation temperatures” and “50% condensation temperatures,” which makes comparisons of volatility somewhat difficult. It should be noted that for some elements condensation temperatures are not known well, if at all. These elements include several alkalis (Rb, Cs), halogens (F, Cl, Br, I), and trace elements (Bi, In, Hg, Pb, Sn, and Tl). More importantly, the different condensation studies used different sets of solar elemental abundances as well as thermodynamic properties, depending on what was available at the time. However, condensation temperatures of the elements

change as solar abundances and thermodynamic properties are revised and updated.

Recently, Allende Prieto, Lambert, & Asplund (2001, 2002) presented substantial downward revisions of the solar abundances of oxygen and carbon compared to previous compilations. Carbon and oxygen are two abundant elements governing much of the chemistry of the other, less abundant elements. A lower absolute oxygen abundance will lower condensation temperatures of O-bearing compounds. In addition to the absolute O abundance, the C/O ratio influences condensation temperatures. The C/O ratio from the determination by Allende Prieto et al. (2001, 2002) is 0.5, which is slightly higher than the C/O ratio of 0.49 found by Grevesse & Sauval (1998), and clearly higher than 0.42 from Anders & Grevesse (1989). An increase in the C/O ratio toward unity lowers the condensation temperatures of oxides and silicates, and the initial oxide and silicate condensates are replaced by C-bearing compounds (e.g., Larimer 1975; Larimer & Bartholomay 1979; Lodders & Fegley 1993; Krot et al. 2000). Changes in abundances of other elements such as sulfur or phosphorus also mean that their condensation temperatures will change.

This paper presents updated solar abundances and self-consistent condensation temperatures for all elements. In § 2, elemental abundances are selected. Data from solar spectroscopy (§ 2.1) and meteoritic analyses (§ 2.2) are used to derive a recommended set of photospheric abundances (§ 2.3), which are then used to derive protosolar (=solar system) abundances in § 2.4. The abundances of the isotopes for the solar system composition are given in § 2.5. The condensation temperatures calculated for the photospheric and solar system abundances are discussed in § 3. Conclusions are given in § 4.

### 2. ELEMENTAL ABUNDANCES

Since 1989, when the widely used elemental abundance table by Anders & Grevesse was published, many revisions

and updates to photospheric and meteoritic abundances of the elements have become available. Updates to the Anders & Grevesse (1989) compilation were made by e.g., Grevesse & Noels (1993), Palme & Beer (1993), Grevesse, Noels, & Sauval (1996), and Grevesse & Sauval (1998, 2002). In these compilations, the solar abundances derived from photospheric and meteoritic data are taken as representative of solar system abundances. (The term “cosmic” abundances, which was used as a synonym for solar system abundances in older literature, is avoided here.) It has been known for some time that abundances determined from lines in the Sun’s photospheric spectrum and abundances in CI-type carbonaceous meteorites agree quite well when normalized to the same scale, with the exception of a few elements. When compared to the photosphere, meteorites are depleted in noble gases and H, C, N, and O, which readily form gaseous compounds, and enriched in elements (e.g., Li) that are processed in the Sun. Of the 83 naturally occurring elements, there are 56 for which a comparison of photospheric and CI chondrite abundances can be done. Excluded from the comparison are elements lighter than fluorine, the noble gases, and elements for which no or only very unreliable photospheric abundance determinations exist (see discussion below). Of the 56 elements for which the comparison can be done, the relative abundances of 31 elements in the photosphere and in CI chondrites agree within 10%; increasing the comparison to within 15% yields agreement for 41 elements. Therefore, the usually more precise analyses of CI chondrites can be used to refine photospheric abundances.

More recently, models of the Sun’s evolution and interior show that currently observed photospheric abundances (relative to hydrogen) must be lower than those of the proto-Sun because helium and other heavy elements have settled toward the Sun’s interior since the time of the Sun’s formation some 4.55 Gyr ago. The abundances of elements heavier than helium apparently did not fractionate relative to each other, but they are fractionated relative to hydrogen (see § 2.3.1.1). Therefore, photospheric abundances relative to hydrogen are not representative of the solar system, and only the protosolar (i.e., unfractionated with respect to hydrogen) abundances represent the “solar system elemental abundances.”

In the following text, “meteoritic” or “CI chondrite” abundances refer to elemental abundances from type CI carbonaceous chondrites, “photospheric” abundances refer to abundance determinations of the present Sun’s photosphere, and “protosolar” or “solar system abundances” refer to elemental abundances of the proto-Sun at the time of its formation.

Two atomic abundance scales are commonly used. The value for an element “El” on the logarithmic astronomical scale is designated as  $A(\text{El}) = \log \epsilon(\text{El})$ . On this scale, the number of H atoms is set to  $A(\text{H}) = \log n(\text{H}) = 12$ , so that

$$A(\text{El}) = \log \epsilon(\text{El}) = \log [n(\text{El})/n(\text{H})] + 12. \quad (1)$$

On the cosmochemical scale, atomic abundances are normalized to the number of silicon atoms of  $N(\text{Si}) = 10^6$ , and abundances on this scale are designated as  $N(\text{El})$ . The photospheric and meteoritic abundances on the two atomic scales are summarized in Table 1, and solar system abundances are given in Table 2.

Uncertainties of photospheric and meteoritic abundance determinations are compared using the relationship  $U(\%) = \pm 100(10^{\pm a} - 1)$ , where  $a$  is the uncertainty in dex units quoted for abundances on the logarithmic scale and  $U$  is the uncertainty on the linear scale in percent. The uncertainty in dex is an uncertainty factor; hence the percent uncertainty is smaller for  $-a$  than for  $+a$ , or vice versa—a given percent uncertainty yields two different uncertainty factors. For a conservative approach, the larger percentage value  $U$  (from a given uncertainty  $a$ ) or the larger uncertainty  $a$  (from a given  $U$ ) is taken for comparison.

### 2.1. Solar Photospheric Abundances

The solar photospheric elemental abundance determinations, which are mainly derived from photospheric lines, are listed in Table 1. This table contains the following information. The chemical symbols for all naturally occurring elements are given in column (1). The recommended elemental abundances for the solar photosphere, derived as described below, are given in astronomical scale [ $A(\text{H}) = 12$ ; col. [2]], and cosmochemical scale [ $N(\text{Si}) = 10^6$ ; col. [3]] atoms. Column (4) indicates how the recommended abundance was selected. Recommended elemental abundances for CI chondrites are listed in columns (5) and (6). These values are derived from Table 3 as discussed in § 2.2. The selected abundances in the solar photosphere are given in columns (7) and (8). The references for the determination or reevaluation of the values listed in column (8) are given in column (9). The years of publication show that many elemental abundances have been (re-)determined relatively recently, but it also shows that the abundances for a few elements (e.g., F, Cl, Rb, Sn, Sb) are those determined almost 30 years ago and that for some elements (As, Se, Br, Te, I, Cs, Ta, Re, Hg, Bi) no photospheric determinations exist because there are no observable lines in the solar spectrum. The abundances of the noble gases He, Ne, Ar, Kr, and Xe cannot be derived from the photospheric spectrum. Ne and Ar abundances can be derived from coronal sources such as solar wind (SW), solar flares, or solar energetic particles (SEP). The He abundance is derived indirectly from results of helioseismology. The abundances of He, Ne, and Ar are described in § 2.3.1. No solar abundance data are available for Kr and Xe; their abundances are derived theoretically. The abundances of F, Cl, and Tl are derived from sunspot spectra (Hall & Noyes 1969, 1972; Lambert, Mallia, & Smith 1972). Photospheric elemental abundances are discussed in the individual papers listed in Table 1 and in various compilations. Notes on some selected elements are combined with the discussion of meteoritic abundances in § 2.3, where the recommended photospheric abundances are described.

### 2.2. CI Chondritic Abundances

Only five CI meteorite falls are known, and of these, only four are massive enough for multiple chemical analyses. Information about these five meteorites is summarized in Table 3. CI chondrites are the most primitive chondrites in the sense that they are not chemically fractionated when relative abundances are compared to the photosphere. However, it should be noted that they are severely altered mineralogically from the “pristine” mineralogy expected for solar nebular condensates. Aqueous alteration on the CI chondrite parent body leads to the formation of hydrous

TABLE 1  
RECOMMENDED ELEMENTAL ABUNDANCES IN THE SOLAR PHOTOSPHERE DERIVED FROM SPECTROSCOPY AND CI CHONDRITES

ELEMENT (1)	RECOMMENDED ABUNDANCE			CI CHONDRITES			SPECTROSCOPY			DATE AND NOTES FOR SPECTROSCOPIC VALUES (9)	REFERENCE (10)
	A(E) (2)	N(E) (3)	SELECTION METHOD <sup>a</sup> (4)	N(E) (5)	A(E) (6)	N(E) (7)	A(E) (8)				
H	≡12	$2.884 \times 10^{10}$	s	$5.498 \times 10^6$	$8.28 \pm 0.05$	$2.884 \times 10^{10}$	≡12	By definition			
He	$10.899 \pm 0.01$	$2.288 \times 10^9$	s	0.6040	1.32	$2.288 \times 10^9$	$10.899 \pm 0.01$	See § 2.3.1.1			
Li	$3.28 \pm 0.06$	55.47	m	55.47	$3.28 \pm 0.06$	0.3631	$1.10 \pm 0.10$	1994		1	
Be	$1.41 \pm 0.08$	0.7374	m	0.7374	$1.41 \pm 0.08$	0.4074	$1.15 \pm 0.20$	1975		2	
B	$2.78 \pm 0.04$	17.32	m	17.32	$2.78 \pm 0.04$	14.45	$2.7^{+0.21} - 0.12$	1999		3	
C	$8.39 \pm 0.04$	$7.079 \times 10^6$	s	$7.724 \times 10^5$	$7.43 \pm 0.06$	$7.079 \times 10^6$	$8.39 \pm 0.04$	2002		4	
N	$7.83 \pm 0.11$	$1.950 \times 10^6$	s	$5.535 \times 10^4$	$6.28 \pm 0.07$	$1.950 \times 10^6$	$7.83 \pm 0.11$	2001, 2002		4, 5	
O	$8.69 \pm 0.05$	$1.413 \times 10^7$	s	$7.552 \times 10^6$	$8.42 \pm 0.02$	$1.413 \times 10^7$	$8.69 \pm 0.05$	2001		6	
F	$4.46 \pm 0.06$	841.1	m	841.1	$4.46 \pm 0.06$	1047	$4.56 \pm 0.30$	1969, sunspot		7	
Ne	$7.87 \pm 0.10$	$2.148 \times 10^6$	s	$2.355 \times 10^{-3}$	-1.09	$2.148 \times 10^6$	$7.87 \pm 0.10$	See § 2.3.1.2		8	
Na	$6.30 \pm 0.03$	$5.751 \times 10^4$	a	$5.747 \times 10^4$	$6.30 \pm 0.03$	$5.754 \times 10^4$	$6.30 \pm 0.03$	1998		5	
Mg	$7.55 \pm 0.02$	$1.020 \times 10^6$	a	$1.040 \times 10^6$	$7.56 \pm 0.02$	$1.000 \times 10^6$	$7.54 \pm 0.06$	2001		9	
Al	$6.46 \pm 0.02$	$8.410 \times 10^4$	a	$8.308 \times 10^4$	$6.46 \pm 0.02$	$8.511 \times 10^4$	$6.47 \pm 0.07$	1984		5	
Si	$7.54 \pm 0.02$	$\equiv 1.000 \times 10^6$	a	$\equiv 1.000 \times 10^6$	$\equiv 7.54 \pm 0.02$	$\equiv 1.000 \times 10^6$	$7.54 \pm 0.05$	2001		10	
P	$5.46 \pm 0.04$	8373	a	7833	$5.43 \pm 0.04$	8913	$5.49 \pm 0.04$	1997		11	
S	$7.19 \pm 0.04$	$4.449 \times 10^5$	m	$4.449 \times 10^5$	$7.19 \pm 0.04$	$4.634 \times 10^5$	$7.20 \pm 0.05$	See § 2.3.4		12	
Cl	$5.26 \pm 0.06$	5237	m	5237	$5.26 \pm 0.06$	9120	$5.5 \pm 0.3$	1972, sunspot		13, 14	
Ar	$6.55 \pm 0.08$	$1.025 \times 10^5$	t	$9.622 \times 10^{-3}$	-0.48	$1.025 \times 10^5$	$6.55 \pm 0.08$	See § 2.3.1.3		15	
K	$5.11 \pm 0.05$	3692	a	3582	$5.09 \pm 0.05$	3802	5.12	1978		16	
Ca	$6.34 \pm 0.03$	$6.287 \times 10^4$	a	$5.968 \times 10^4$	$6.32 \pm 0.03$	$6.607 \times 10^4$	$6.36 \pm 0.02$	1984		17	
Sc	$3.07 \pm 0.04$	34.20	m	34.20	$3.07 \pm 0.04$	42.66	$3.17 \pm 0.10$	1993		18	
Ti	$4.92 \pm 0.03$	2422	m	2422	$4.92 \pm 0.03$	3020	$5.02 \pm 0.06$	1996		19	
V	$4.00 \pm 0.03$	288.4	a	288.4	$4.00 \pm 0.03$	288.4	$4.00 \pm 0.02$	1989		20	
Cr	$5.65 \pm 0.05$	$1.286 \times 10^4$	a	$1.313 \times 10^4$	$5.66 \pm 0.05$	$1.259 \times 10^4$	$5.64 \pm 0.13$	1978		21	
Mn	$5.50 \pm 0.03$	9168	m	9168	$5.50 \pm 0.03$	7079	$5.39 \pm 0.03$	1984		22	
Fe	$7.47 \pm 0.03$	$8.380 \times 10^5$	a	$8.632 \times 10^5$	$7.48 \pm 0.03$	$8.128 \times 10^5$	$7.45 \pm 0.08$	2001		23	
Co	$4.91 \pm 0.03$	2323	a	2246	$4.89 \pm 0.03$	2399	$4.92 \pm 0.08$	1982		24	
Ni	$6.22 \pm 0.03$	$4.780 \times 10^4$	a	$4.780 \times 10^4$	$6.22 \pm 0.03$	$4.780 \times 10^4$	$6.22 \pm 0.13$	1980		25	
Cu	$4.26 \pm 0.06$	527.0	m	527.0	$4.26 \pm 0.06$	467.7	$4.21 \pm 0.04$	1989		26	
Zn	$4.63 \pm 0.04$	1226	a	1250	$4.64 \pm 0.04$	1202	$4.62 \pm 0.15$	1988		27	
Ga	$3.10 \pm 0.06$	35.97	m	35.97	$3.10 \pm 0.06$	21.88	$2.88 \pm 0.10$	1984, 1989		28	
Ge	$3.62 \pm 0.05$	120.6	m	120.6	$3.62 \pm 0.05$	109.6	$3.58 \pm 0.05$	1999		29	
As	$2.32 \pm 0.05$	6.089	m	6.089	$2.32 \pm 0.05$	...	...	...		30	
Se	$3.36 \pm 0.04$	65.79	m	65.79	$3.36 \pm 0.04$	...	...	...		31	
Br	$2.59 \pm 0.09$	11.32	m	11.32	$2.59 \pm 0.09$	...	...	...		32	
Kr	$3.28 \pm 0.08$	55.15	t	$1.643 \times 10^{-4}$	-2.24	55.15	$3.28 \pm 0.08$	1993, see § 2.3.1.4		33	
Rb	$2.36 \pm 0.06$	6.572	m	6.572	$2.36 \pm 0.06$	11.48	2.60	1972		34	
Sr	$2.91 \pm 0.04$	23.64	a	23.30	$2.91 \pm 0.04$	23.99	$2.92 \pm 0.05$	2000		35	
Y	$2.20 \pm 0.03$	4.608	a	4.538	$2.20 \pm 0.04$	4.677	$2.21 \pm 0.02$	1994		36	
Zr	$2.60 \pm 0.03$	11.33	a	11.45	$2.60 \pm 0.02$	11.22	$2.59 \pm 0.04$	1994		37	
Nb	$1.42 \pm 0.03$	0.7554	a	0.7522	$1.42 \pm 0.03$	0.7586	$1.42 \pm 0.06$	1985		38	
Mo	$1.96 \pm 0.04$	2.601	a	2.804	$1.99 \pm 0.04$	2.399	$1.92 \pm 0.05$	1983		39	
Ru	$1.82 \pm 0.08$	1.900	a	1.806	$1.80 \pm 0.08$	1.995	$1.84 \pm 0.07$	1984		40	
Rh	$1.11 \pm 0.03$	0.3708	a	0.3613	$1.10 \pm 0.02$	0.3802	$1.12 \pm 0.12$	1982		41	
Pd	$1.70 \pm 0.03$	1.435	a	1.457	$1.70 \pm 0.02$	1.413	$1.69 \pm 0.04$	1982		42	
Ag	$1.23 \pm 0.06$	0.4913	m	0.4913	$1.23 \pm 0.06$	(0.251)	(0.94)	1984		43	
Cd	$1.74 \pm 0.03$	1.584	m	1.584	$1.74 \pm 0.03$	1.698	$1.77 \pm 0.11$	1990		44	

TABLE 1—Continued

ELEMENT (1)	RECOMMENDED ABUNDANCE		SELECTION METHOD <sup>a</sup> (4)	CI CHONDRITES		SPECTROSCOPY		DATE AND NOTES FOR SPECTROSCOPIC VALUES		REFERENCE (10)
	A(EI) (2)	N(EI) (3)		N(EI) (5)	A(EI) (6)	N(EI) (7)	A(EI) (8)	(9)		
In	0.80 ± 0.03	0.1810	m	0.1810	0.80 ± 0.03	1.047	1.56 ± 0.2	2002	33	
Sn	2.11 ± 0.04	3.733	m	3.733	2.11 ± 0.04	2.884	2.0 ± 0.3	1976	34	
Sb	1.06 ± 0.07	0.3292	m	0.3292	1.06 ± 0.07	0.2884	1.0 ± 0.3	1976	34	
Te	2.22 ± 0.04	4.815	m	4.815	2.22 ± 0.04	...	...	...	...	
I	1.54 ± 0.12	0.9975	m	0.9975	1.54 ± 0.12	...	...	...	...	
Xe	2.27 ± 0.02	5.391	t	3.495 × 10 <sup>-4</sup>	-1.92	5.391	2.27 ± 0.02	2002, see § 2.3.1.4	35	
Cs	1.10 ± 0.03	0.3671	m	0.3671	1.10 ± 0.03	...	...	...	...	
Ba	2.18 ± 0.03	4.351	a	4.436	2.19 ± 0.03	4.266	2.17 ± 0.07	1994	27	
La	1.18 ± 0.06	0.4405	m	0.4405	1.18 ± 0.06	0.3890	1.13 ± 0.03	2001	36	
Ce	1.61 ± 0.02	1.169	m	1.169	1.61 ± 0.02	1.096	1.58 ± 0.09	1994	27	
Pr	0.78 ± 0.03	0.1737	m	0.1737	0.78 ± 0.03	0.1479	0.71 ± 0.08	1979	37	
Nd	1.46 ± 0.03	0.8355	m	0.8355	1.46 ± 0.03	0.912	1.50 ± 0.12	1985	38	
Sm	0.95 ± 0.04	0.2542	m	0.2542	0.95 ± 0.04	0.2818	0.99	1994	27	
Eu	0.52 ± 0.04	0.09513	a	0.09475	0.52 ± 0.04	0.09550	0.52 ± 0.04	2001	39	
Gd	1.06 ± 0.02	0.3321	m	0.3321	1.06 ± 0.02	0.3802	1.12 ± 0.04	1988	40	
Tb	0.31 ± 0.03	0.05907	m	0.05907	0.31 ± 0.03	0.05495	0.28 ± 0.30	2001	41	
Dy	1.13 ± 0.04	0.3862	m	0.3862	1.13 ± 0.04	0.3981	1.14 ± 0.08	1993	42	
Ho	0.49 ± 0.02	0.08986	m	0.08986	0.49 ± 0.02	0.09772	0.53 ± 0.10	2002	33	
Er	0.95 ± 0.03	0.2554	m	0.2554	0.95 ± 0.03	0.2455	0.93 ± 0.06	1984	43	
Tm	0.11 ± 0.06	0.03700	m	0.03700	0.11 ± 0.06	(0.0288)	(0.00 ± 0.15)	1984	9	
Yb	0.94 ± 0.03	0.2484	m	0.2484	0.94 ± 0.03	0.3467	1.08 ± 0.15	1984, 1989	9, 21	
Lu	0.09 ± 0.06	0.03572	m	0.03572	0.09 ± 0.06	0.03311	0.06 ± 0.10	1998	44	
Hf	0.77 ± 0.04	0.1699	m	0.1699	0.77 ± 0.04	0.2188	0.88 ± 0.08	1976	45	
Ta	-0.14 ± 0.03	0.02099	m	0.02099	-0.14 ± 0.03	...	...	...	...	
W	0.65 ± 0.03	0.1277	m	0.1277	0.65 ± 0.03	(0.372)	(1.11 ± 0.15)	1984	9	
Re	0.26 ± 0.04	0.05254	m	0.05254	0.26 ± 0.04	...	...	...	...	
Os	1.37 ± 0.03	0.6738	m	0.6738	1.37 ± 0.03	0.8128	1.45 ± 0.10	1984	46	
Ir	1.35 ± 0.03	0.6448	m	0.6448	1.35 ± 0.03	0.6918	1.38 ± 0.05	1988	47	
Pt	1.67 ± 0.03	1.357	m	1.357	1.67 ± 0.03	1.585	1.74	1987	48	
Au	0.83 ± 0.06	0.1955	m	0.1955	0.83 ± 0.06	(0.295)	(1.01)	1989	21	
Hg	1.16 ± 0.18	0.4128	m	0.4128	1.16 ± 0.18	...	...	See § 2.3.6	...	
Tl	0.81 ± 0.04	0.1845	m	0.1845	0.81 ± 0.04	(0.15-0.36)	(0.72-1.10)	1972, sunspot	49	
Pb	2.05 ± 0.04	3.258	m	3.258	2.05 ± 0.04	2.884	2.00 ± 0.06	2000	50	
Bi	0.68 ± 0.03	0.1388	m	0.1388	0.68 ± 0.03	...	...	...	...	
Th	0.09 ± 0.04	0.03512	m	0.03512	0.09 ± 0.04	...	...	1996, blended line	15	
U	-0.49 ± 0.04	9.306 × 10 <sup>-3</sup>	m	9.306 × 10 <sup>-3</sup>	-0.49 ± 0.04	<9.772 × 10 <sup>-3</sup>	<-0.47	1984	9	

NOTE.—See text for detailed description of table. Data in parentheses are uncertain. Mass fractions in photosphere:  $X = 0.7491$ ,  $Y = 0.2377$ ,  $Z = 0.0133$ ;  $Z/X = 0.0177$ . The astronomical log scale and the cosmochemical abundance scale by number are coupled by  $A(EI) = \log[N(EI)] + 1.540$ .

<sup>a</sup> Recommended photospheric value from s = spectroscopy, m = meteoritic, a = average of spectroscopy and CI chondrites, t = theoretical value.

REFERENCES.—(1) Carlsson et al. 1994; (2) Chiemelewski et al. 1975; (3) Cunha & Smith 1999; (4) Allende Prieto et al. 2002; (5) Holweger 2001; (6) Allende Prieto et al. 2001; (7) Hall & Noyes 1969; (8) Baumüller, Butler, & Gehren 1998; (9) Grevesse 1984; (10) Berzonsh, Svanberg, & Biémont 1997; (11) Hall & Noyes 1972; (12) Lambert & Luck 1978; (13) Grevesse & Noels 1993; (14) Neuforge 1993; (15) Grevesse et al. 1996; (16) Biémont et al. 1989; (17) Biémont, Grevesse, & Huber 1978; (18) Booth, Blackwell, & Shalilis 1984; (19) Cardon et al. 1982; (20) Biémont et al. 1980; (21) Anders & Grevesse 1989; (22) Sneden & Crocker 1988; (23) Biémont et al. 1999; (24) Palme & Beer 1993; (25) Hauge 1972; (26) Barklem & O'Mara 2000; (27) Gratton & Sneden 1994; (28) Hannaford et al. 1985; (29) Biémont et al. 1983; (30) Biémont et al. 1984; (31) Kwiatkowski et al. 1982; (32) Youssef, Dönszelmann, & Grevesse 1990; (33) Bord & Cowley 2002; (34) Ross & Aller 1976; (35) Reifarth et al. 2002; (36) Lawler, Bonvallet, & Sneden 2001; (37) Biémont, Grevesse, & Hauge 1979; (38) Ward et al. 1985; (39) Lawler et al. 2001b; (40) Bergström et al. 1988; (41) Lawler et al. 2001a; (42) Grevesse, Noels, & Sauval 1993; (43) Biémont & Youssef 1984; (44) Bord, Cowley, & Mirijanian 1998; (45) Andersen, Petersen, & Hauge 1976; (46) Kwiatkowski et al. 1984; (47) Youssef & Khalil 1988; (48) Youssef & Khalil 1987; (49) Lambert, Mallia, & Smith 1972; (50) Biémont et al. 2000.



TABLE 2  
RECOMMENDED ELEMENTAL ABUNDANCES OF THE PROTO-SUN (SOLAR SYSTEM ABUNDANCES)

Element	$A(\text{El})_0$	$N(\text{El})_0$	Element	$A(\text{El})_0$	$N(\text{El})_0$	Element	$A(\text{El})_0$	$N(\text{El})_0$
H .....	$\equiv 12$	$2.431 \times 10^{10}$	Ge .....	$3.70 \pm 0.05$	120.6	Sm .....	$1.02 \pm 0.04$	0.2542
He .....	$10.984 \pm 0.02$	$2.343 \times 10^9$	As .....	$2.40 \pm 0.05$	6.089	Sm* .....	$1.02 \pm 0.04$	0.2554
Li .....	$3.35 \pm 0.06$	55.47	Se .....	$3.43 \pm 0.04$	65.79	Eu .....	$0.60 \pm 0.04$	0.09513
Be .....	$1.48 \pm 0.08$	0.7374	Br .....	$2.67 \pm 0.09$	11.32	Gd .....	$1.13 \pm 0.02$	0.3321
B .....	$2.85 \pm 0.04$	17.32	Kr .....	$3.36 \pm 0.08$	55.15	Tb .....	$0.38 \pm 0.03$	0.05907
C .....	$8.46 \pm 0.04$	$7.079 \times 10^6$	Rb .....	$2.43 \pm 0.06$	6.572	Dy .....	$1.21 \pm 0.04$	0.3862
N .....	$7.90 \pm 0.11$	$1.950 \times 10^6$	Rb* .....	$2.44 \pm 0.06$	6.694	Ho .....	$0.56 \pm 0.02$	0.08986
O .....	$8.76 \pm 0.05$	$1.413 \times 10^7$	Sr .....	$2.99 \pm 0.04$	23.64	Er .....	$1.02 \pm 0.03$	0.2554
F .....	$4.53 \pm 0.06$	841.1	Sr* .....	$2.99 \pm 0.04$	23.52	Tm .....	$0.18 \pm 0.06$	0.03700
Ne .....	$7.95 \pm 0.10$	$2.148 \times 10^6$	Y .....	$2.28 \pm 0.03$	4.608	Yb .....	$1.01 \pm 0.03$	0.2484
Na .....	$6.37 \pm 0.03$	$5.751 \times 10^4$	Zr .....	$2.67 \pm 0.03$	11.33	Lu .....	$0.16 \pm 0.06$	0.03572
Mg .....	$7.62 \pm 0.02$	$1.020 \times 10^6$	Nb .....	$1.49 \pm 0.03$	0.7554	Lu* .....	$0.17 \pm 0.06$	0.03580
Al .....	$6.54 \pm 0.02$	$8.410 \times 10^4$	Mo .....	$2.03 \pm 0.04$	2.601	Hf .....	$0.84 \pm 0.04$	0.1699
Si .....	$7.61 \pm 0.02$	$\equiv 1.00 \times 10^6$	Ru .....	$1.89 \pm 0.08$	1.900	Hf* .....	$0.84 \pm 0.04$	0.1698
P .....	$5.54 \pm 0.04$	8373	Rh .....	$1.18 \pm 0.03$	0.3708	Ta .....	$-0.06 \pm 0.03$	0.02099
S .....	$7.26 \pm 0.04$	$4.449 \times 10^5$	Pd .....	$1.77 \pm 0.03$	1.435	W .....	$0.72 \pm 0.03$	0.1277
Cl .....	$5.33 \pm 0.06$	5237	Ag .....	$1.30 \pm 0.06$	0.4913	Re .....	$0.33 \pm 0.04$	0.05254
Ar .....	$6.62 \pm 0.08$	$1.025 \times 10^5$	Cd .....	$1.81 \pm 0.03$	1.584	Re* .....	$0.36 \pm 0.04$	0.05509
K .....	$5.18 \pm 0.05$	3692	In .....	$0.87 \pm 0.03$	0.1810	Os .....	$1.44 \pm 0.03$	0.6738
K* .....	$5.18 \pm 0.05$	3697	Sn .....	$2.19 \pm 0.04$	3.733	Os* .....	$1.44 \pm 0.03$	0.6713
Ca .....	$6.41 \pm 0.03$	$6.287 \times 10^4$	Sb .....	$1.14 \pm 0.07$	0.3292	Ir .....	$1.42 \pm 0.03$	0.6448
Sc .....	$3.15 \pm 0.04$	34.20	Te .....	$2.30 \pm 0.04$	4.815	Pt .....	$1.75 \pm 0.03$	1.357
Ti .....	$5.00 \pm 0.03$	2422	I .....	$1.61 \pm 0.12$	0.9975	Au .....	$0.91 \pm 0.06$	0.1955
V .....	$4.07 \pm 0.03$	288.4	Xe .....	$2.35 \pm 0.02$	5.391	Hg .....	$1.23 \pm 0.18$	0.4128
Cr .....	$5.72 \pm 0.05$	$1.286 \times 10^4$	Cs .....	$1.18 \pm 0.03$	0.3671	Tl .....	$0.88 \pm 0.04$	0.1845
Mn .....	$5.58 \pm 0.03$	9168	Ba .....	$2.25 \pm 0.03$	4.351	Pb .....	$2.13 \pm 0.04$	3.258
Fe .....	$7.54 \pm 0.03$	$8.380 \times 10^5$	La .....	$1.25 \pm 0.06$	0.4405	Pb* .....	$2.12 \pm 0.04$	3.234
Co .....	$4.98 \pm 0.03$	2323	Ce .....	$1.68 \pm 0.02$	1.169	Bi .....	$0.76 \pm 0.03$	0.1388
Ni .....	$6.29 \pm 0.03$	$4.780 \times 10^4$	Pr .....	$0.85 \pm 0.03$	0.1737	Th .....	$0.16 \pm 0.04$	0.03512
Cu .....	$4.34 \pm 0.06$	527.0	Nd .....	$1.54 \pm 0.03$	0.8355	Th* .....	$0.26 \pm 0.04$	0.04399
Zn .....	$4.70 \pm 0.04$	1226	Nd* .....	$1.54 \pm 0.03$	0.8343	U .....	$-0.42 \pm 0.04$	$9.306 \times 10^{-3}$
Ga .....	$3.17 \pm 0.06$	35.97				U* .....	$+0.01 \pm 0.04$	$24.631 \times 10^{-3}$

NOTE.—Values for elements marked with an asterisk are abundances  $4.55 \times 10^9$  yr ago. Mass fractions for proto-Sun:  $X_0 = 0.7110$ ,  $Y_0 = 0.2741$ ,  $Z_0 = 0.0149$ , and  $X_0/Z_0 = 0.0210$ . The astronomical log scale and the cosmochemical abundance scale by number are coupled by  $A(\text{El})_0 = \log[N(\text{El})] + 1.614$ .

silicates and carbonates and to magnetite formation from metal. This alteration must occur in a closed chemical system because overall relative elemental abundances of rocky elements are preserved. Indeed, chondrules are essentially absent from CI chondrites, which are only called “chondrites” because of their unfractionated elemental abundances. However, aqueous alteration likely has led to redistribution of some elements such as S, Ca, and Mn within the CI chondrite parent body, and abundance determinations for some elements may have statistically larger uncertainties, which simply reflect sample heterogeneity introduced by parent body alterations.

Here it should be noted that chondritic meteorites in their present form are not unaltered equilibrium condensates from the solar nebula. Chondrites have experienced mineralogical alterations by thermal metamorphism, and in the case of CI and CM chondrites, also by aqueous alteration on their parent bodies. However, the chondrite parent bodies themselves must have accumulated from nebular condensates. Assuming that the parent body alterations occurred in a closed system, the *chemical* composition then still remains that of the nebular condensates accreted by the chondritic meteorite parent bodies. However, some individual phases, such as calcium-aluminum-rich inclusions in chondrites, may represent more or less unaltered condensates (see § 3.2).

More analytical data are available for the Orgueil meteorite, the most massive of the CI chondrites, than for any of the others. Previous compilations (e.g., Anders & Grevesse 1989; Palme & Beer 1993) therefore give preference to the Orgueil data in selecting the solar system abundances based on meteorites. Here the CI chondrite group-mean composition was determined as follows. For each CI chondrite, elemental analyses were collected from the literature. The data sources include those given by Anders & Ebihara (1982), Anders & Grevesse (1989), Palme & Beer (1993), and literature data published since then. Where relevant, literature sources are discussed in § 2.3. Mean elemental concentrations (by mass) for each meteorite were computed from all reliable analytical data. The resulting elemental means for each meteorite are listed in Table 3, together with  $1 \sigma$  standard deviations and the number of analyses ( $N$ ) included in the mean.

The CI chondrite group-mean composition (last columns in Table 3) was obtained by taking the weighted average of the compositions from the individual meteorites, using the number of analyses ( $N$ ) as statistical weight. The uncertainties given are the square root of the weighted variance of the weighted average. Values in parenthesis in Table 3 are not included in the computation of the group mean. Several elements (e.g., Mg, Ca, Mn, Cr, Na, and K) have larger uncertainties in individual chondrites than calculated for the

TABLE 3  
ELEMENTAL ABUNDANCES IN CI CHONDRITES

ELEMENT	ALAIS		IVUNA		ORGUEIL		REVELSTOKE		TONK		CI CHONDRITE GROUP	
	Mean $\pm 1\sigma$	N	Mean $\pm 1\sigma$	N	Mean $\pm 1\sigma$	N	Mean	N	Mean $\pm 1\sigma$	N	Weighted Mean $\pm 1\sigma$	N <sub>net</sub>
H	21800	1	20900	1	19730 $\pm$ 2270	3	...	...	24200	1	21015 $\pm$ 1770	4
He	...		...		9.17 $\times 10^{-3}$	6	...	...	...		9.17 $\times 10^{-3}$	See § 2.3.1.5
Li	...		1.52	1	1.45 $\pm$ 0.21	(1)	...	...	...		1.46 $\pm$ 0.03	2
Be	...		...		(0.019)	2	...	...	...		0.0252 $\pm$ 0.005	See § 2.3.2.1
B	0.650 $\pm$ 0.028	2	0.650 $\pm$ 0.028	2	0.775 $\pm$ 0.007	2	...	...	...		0.713 $\pm$ 0.072	2, § 2.3.2.2
C	29450 $\pm$ 3465	2	44300 $\pm$ 5660	2	34800 $\pm$ 4585	9	40000	1	27000	1	35180 $\pm$ 4810	5
N	2900	1	...		2948 $\pm$ 535	5	...	...	...		2940 $\pm$ 20	2
O	(47170)	a	454,130	a	462,250	a	(413,400)	a	(488,700)	a	458,200 $\pm$ 5750	2
F	...		66.5 $\pm$ 4.9	2	58.2 $\pm$ 9.3	5	...	...	...		60.6 $\pm$ 4.1	2
Ne	...		...		1.80 $\times 10^{-4}$	5	...	...	...		1.80 $\times 10^{-4}$	See § 2.3.1.5
Na	5060 $\pm$ 316	4	5070 $\pm$ 390	3	4990 $\pm$ 380	20	...	...	(5660)	(1)	5010 $\pm$ 33	3
Mg	94170 $\pm$ 3260	3	97100 $\pm$ 655	3	95950 $\pm$ 4400	17	(120,000)	(1)	(82700)	(1)	95870 $\pm$ 780	3
Al	8230 $\pm$ 275	5	8475 $\pm$ 210	6	8580 $\pm$ 480	18	(2200)	(1)	(10200)	(1)	8500 $\pm$ 130	3
Si	(97100)	(1)	108,300 $\pm$ 3200	5	105,700 $\pm$ 2800	11	(130,000)	(1)	(104,700)	(1)	106,500 $\pm$ 1250	2
P	(1200)	(1)	(760)	(1)	924 $\pm$ 100	8	...	...	(480)	(1)	920 $\pm$ 100	1
S	64600	1	50820 $\pm$ 5050	3	53500 $\pm$ 2530	7	54000	1	58000	1	54100 $\pm$ 3650	5
Cl	...		724 $\pm$ 37	2	700 $\pm$ 110	9	...	...	(510)	(1)	704 $\pm$ 10	2
Ar	...		...		1.33 $\times 10^{-3}$	9	...	...	...		1.33 $\times 10^{-3}$	See § 2.3.1.5
K	524 $\pm$ 57	2	475 $\pm$ 18	3	543 $\pm$ 35	17	(800)	(1)	510	1	530 $\pm$ 24	4
Ca	9030 $\pm$ 380	3	(9700)	(1)	9076 $\pm$ 656	14	(11000)	(1)	9050 $\pm$ 780	2	9070 $\pm$ 20	3
Sc	5.79 $\pm$ 0.23	2	5.74 $\pm$ 0.48	3	5.84 $\pm$ 0.49	13	...	...	6	1	5.83 $\pm$ 0.06	4
Ti	450	1	440 $\pm$ 28	2	439 $\pm$ 30	15	(1000)	(1)	(540)	(1)	440 $\pm$ 3	3
V	52.5 $\pm$ 3.5	2	58.0	1	56.0 $\pm$ 3.7	13	...	...	...		55.7 $\pm$ 1.3	3
Cr	2470 $\pm$ 320	3	2460 $\pm$ 149	3	2630 $\pm$ 150	16	(3200)	(1)	2690	1	2590 $\pm$ 80	4
Mn	1940 $\pm$ 150	4	1823 $\pm$ 84	4	1920 $\pm$ 100	16	(2500)	(1)	(1400)	(1)	1910 $\pm$ 40	3
Fe	178,200 $\pm$ 720	3	182,500 $\pm$ 12300	7	183,470 $\pm$ 7900	24	(220,000)	(1)	182,150 $\pm$ 1910	2	182,800 $\pm$ 1470	4
Co	518 $\pm$ 25	4	468 $\pm$ 31	5	507 $\pm$ 24	19	...	...	(330)	(1)	502 $\pm$ 17	3
Ni	10100 $\pm$ 252	5	10910 $\pm$ 600	7	10670 $\pm$ 640	33	(600)	(1)	(770 $\pm$ 35)	(2)	10640 $\pm$ 210	3
Cu	130	1	118 $\pm$ 16	5	131 $\pm$ 21	11	(13000)	(1)	130	1	127 $\pm$ 6	4
Zn	301 $\pm$ 6	4	293 $\pm$ 26	10	318 $\pm$ 26	30	...	...	280	1	310 $\pm$ 12	4
Ga	9.60	2	8.87 $\pm$ 1.34	3	9.57 $\pm$ 0.68	15	...	...	10.3	1	9.51 $\pm$ 0.31	4
Ge	33.9 $\pm$ 3.7	4	33.1 $\pm$ 2.0	6	33.1 $\pm$ 2.7	18	...	...	...		33.2 $\pm$ 0.3	3
As	1.82 $\pm$ 0.04	2	1.77 $\pm$ 0.21	3	1.70 $\pm$ 0.23	18	...	...	1.95	1	1.73 $\pm$ 0.06	4
Se	20.5 $\pm$ 0.9	4	20.0 $\pm$ 1.1	8	19.5 $\pm$ 1.9	26	...	...	21	1	19.7 $\pm$ 0.4	4
Br	2.35 $\pm$ 0.08	3	4.82 $\pm$ 0.75	6	3.18 $\pm$ 0.56	21	...	...	(9)	(1)	3.43 $\pm$ 0.75	3
Kr	...		...		5.22 $\times 10^{-5}$	21	...	...	...		5.22 $\times 10^{-5}$	See § 2.3.1.5
Rb	(1.55 $\pm$ 0.04)	(2)	2.16 $\pm$ 0.32	15	2.12 $\pm$ 0.31	30	...	( $<$ 4)	...	(1)	2.13 $\pm$ 0.02	2
Sr	...		7.89 $\pm$ 0.75	7	7.67 $\pm$ 0.56	16	...	...	...		7.74 $\pm$ 0.10	2
Y	...		1.35 $\pm$ 0.14	4	1.60 $\pm$ 0.14	10	...	...	...		1.53 $\pm$ 0.12	2
Zr	...		3.77 $\pm$ 0.22	4	4.02 $\pm$ 0.23	12	...	...	...		3.96 $\pm$ 0.11	2
Nb	...		0.30	1	0.259 $\pm$ 0.015	6	...	...	...		0.265 $\pm$ 0.016	2
Mo	...		1.12 $\pm$ 0.08	3	0.929 $\pm$ 0.036	3	...	...	...		1.02 $\pm$ 0.11	2
Ru	0.662	1	0.633 $\pm$ 0.124	4	0.725 $\pm$ 0.032	8	...	...	(0.94)	(1)	0.692 $\pm$ 0.044	3
Rh	...		0.142 $\pm$ 0.002	2	0.139 $\pm$ 0.002	2	...	...	...		0.141 $\pm$ 0.002	2
Pd	0.557	1	0.557 $\pm$ 0.027	6	0.600 $\pm$ 0.034	17	...	...	...		0.588 $\pm$ 0.020	3
Ag	0.204	1	0.194 $\pm$ 0.031	5	0.203 $\pm$ 0.018	16	...	...	...		0.201 $\pm$ 0.004	3

TABLE 3—Continued

ELEMENT	ALAIS		IVUNA		ORQUEIL		REVELSTOKE		TONK		CI CHONDRITE GROUP	
	Mean $\pm 1\sigma$	<i>N</i>	Mean $\pm 1\sigma$	<i>N</i>	Mean $\pm 1\sigma$	<i>N</i>	Mean	<i>N</i>	Mean $\pm 1\sigma$	<i>N</i>	Weighted Mean $\pm 1\sigma$	<i>N</i> <sub>net</sub>
Cd.....	0.657 $\pm$ 0.042	3	0.683 $\pm$ 0.031	6	0.675 $\pm$ 0.046	25	...	...	...	...	0.675 $\pm$ 0.006	3
In.....	0.0838 $\pm$ 0.0006	2	0.080 $\pm$ 0.006	4	0.0779 $\pm$ 0.0043	17	...	...	...	...	0.0788 $\pm$ 0.002	3
Sn.....	1.80	1	1.72 $\pm$ 0.11	3	1.663 $\pm$ 0.160	12	...	...	...	...	1.68 $\pm$ 0.04	3
Sb.....	0.181 $\pm$ 0.01	3	0.158 $\pm$ 0.029	7	0.148 $\pm$ 0.026	29	...	...	(0.12)	(1)	0.152 $\pm$ 0.009	3
Te.....	2.89 $\pm$ 0.29	2	2.34 $\pm$ 0.22	4	2.26 $\pm$ 0.17	17	...	...	...	...	2.33 $\pm$ 0.18	3
I.....	...	...	(1.12 $\pm$ 0.51)	(4)	0.48 $\pm$ 0.16	6	...	...	...	...	0.48 $\pm$ 0.16	1
Xe.....	...	...	...	...	1.74 $\times 10^{-4}$	...	...	...	...	...	1.74 $\times 10^{-4}$	See § 2.3.1.5
Cs.....	0.181 $\pm$ 0.011	2	0.187 $\pm$ 0.012	10	0.184 $\pm$ 0.012	17	...	...	...	...	0.185 $\pm$ 0.002	3
Ba.....	...	...	2.36	1	2.30 $\pm$ 0.14	5	...	...	...	...	2.31 $\pm$ 0.03	2
La.....	0.218 $\pm$ 0.007	2	0.211 $\pm$ 0.029	2	0.238 $\pm$ 0.020	14	...	...	0.22	1	0.232 $\pm$ 0.010	4
Ce.....	0.579	1	0.602 $\pm$ 0.014	3	0.637 $\pm$ 0.025	6	...	...	...	...	0.621 $\pm$ 0.022	3
Pr.....	...	...	0.0935 $\pm$ 0.0050	2	0.0925 $\pm$ 0.0059	4	...	...	...	...	0.0928 $\pm$ 0.0005	2
Nd.....	0.489	1	0.447 $\pm$ 0.037	5	0.459 $\pm$ 0.021	9	...	...	...	...	0.457 $\pm$ 0.011	3
Sm.....	0.148 $\pm$ 0.004	2	0.143 $\pm$ 0.008	3	0.145 $\pm$ 0.015	17	...	...	0.15	1	0.145 $\pm$ 0.002	4
Eu.....	0.0556 $\pm$ 0.0020	3	0.0528 $\pm$ 0.0038	3	0.0548 $\pm$ 0.0044	15	...	...	0.053	1	0.0546 $\pm$ 0.0010	4
Gd.....	...	...	0.187 $\pm$ 0.010	2	0.201 $\pm$ 0.011	8	...	...	...	...	0.198 $\pm$ 0.006	2
Tb.....	0.0369	1	0.0310	1	0.0372 $\pm$ 0.0026	2	...	...	...	...	0.0356 $\pm$ 0.0031	3
Dy.....	...	...	0.235 $\pm$ 0.006	2	0.239 $\pm$ 0.021	9	...	...	(0.2)	(1)	0.238 $\pm$ 0.002	2
Ho.....	...	...	0.0580	2	0.0555 $\pm$ 0.0023	5	...	...	...	...	0.0562 $\pm$ 0.0012	2
Er.....	...	...	0.152 $\pm$ 0.005	3	0.167 $\pm$ 0.012	6	...	...	...	...	0.162 $\pm$ 0.008	2
Tm.....	...	...	0.0220	1	0.0245 $\pm$ 0.0035	2	...	...	...	...	0.0237 $\pm$ 0.0014	2
Yb.....	0.166 $\pm$ 0.019	3	0.152 $\pm$ 0.026	4	0.165 $\pm$ 0.013	15	...	...	0.16	1	0.163 $\pm$ 0.005	4
Lu.....	0.0240 $\pm$ 0.0018	2	0.0240	2	0.0235 $\pm$ 0.0030	11	...	...	0.024	1	0.0237 $\pm$ 0.0002	4
Hf.....	...	...	0.10	1	0.116 $\pm$ 0.010	7	...	...	0.12	1	0.115 $\pm$ 0.006	3
Ta.....	...	...	0.0143	1	0.0145 $\pm$ 0.0010	2	...	...	...	...	0.0144 $\pm$ 0.0001	2
W.....	...	...	...	...	0.089 $\pm$ 0.007	5	...	...	...	...	0.089 $\pm$ 0.007	1
Re.....	0.0333 $\pm$ 0.0026	2	0.0350 $\pm$ 0.0017	3	0.0379 $\pm$ 0.0035	18	...	...	(0.055)	(1)	0.037 $\pm$ 0.002	3
Os.....	0.469 $\pm$ 0.027	3	0.491 $\pm$ 0.010	2	0.487 $\pm$ 0.033	20	...	...	0.5	1	0.486 $\pm$ 0.007	4
Ir.....	0.458 $\pm$ 0.026	4	0.481 $\pm$ 0.029	4	0.470 $\pm$ 0.029	31	...	...	0.46	1	0.470 $\pm$ 0.005	4
Pt.....	(0.6)	(1)	1.095 $\pm$ 0.055	6	0.962 $\pm$ 0.075	13	...	...	(1.2)	(1)	1.004 $\pm$ 0.064	2
Au.....	(0.103 $\pm$ 0.01)	(5)	0.148 $\pm$ 0.021	8	0.145 $\pm$ 0.015	29	...	...	...	...	0.146 $\pm$ 0.002	2
Hg.....	...	...	0.293 $\pm$ 0.106	3	0.345 $\pm$ 0.191	2	...	...	...	...	0.314 $\pm$ 0.029	2, see § 2.3.6
Tl.....	0.140 $\pm$ 0.006	2	0.140 $\pm$ 0.012	3	0.144 $\pm$ 0.011	13	...	...	...	...	0.143 $\pm$ 0.002	3
Pb.....	...	...	2.52 $\pm$ 0.18	3	2.584 $\pm$ 0.257	4	...	...	...	...	2.56 $\pm$ 0.03	2
Bi.....	(0.166 $\pm$ 0.031)	(2)	0.114 $\pm$ 0.007	6	0.108 $\pm$ 0.009	13	...	...	...	...	0.110 $\pm$ 0.003	2
Th.....	0.0387 $\pm$ 0.0016	2	0.0286 $\pm$ 0.0011	8	0.0312 $\pm$ 0.0021	7	...	...	0.0313 $\pm$ 0.0004	2	0.0309 $\pm$ 0.003	4
U.....	0.0095 $\pm$ 0.0006	3	0.0080 $\pm$ 0.0005	8	0.0081 $\pm$ 0.0004	14	...	...	0.0107 $\pm$ 0.0012	2	0.0084 $\pm$ 0.008	4

NOTE.—ppm by mass =  $\mu\text{g g}^{-1}$ . Date of meteorite fall and known mass: Alais: 1806 Mar 15, 6 kg; Ivuna: 1938 Dec 16, 0.7 kg; Orgueil: 1864 May 14, 14 kg; Revelstoke: 1965 Mar 31, 1 g; Tonk: 1911 Jan 22, 10 g. *N* = number of analyses included in mean; *N*<sub>net</sub> = number of meteorites included in weighted group mean. Elemental abundances given in parentheses are excluded in the group mean. <sup>a</sup> Oxygen abundance by difference to 100%.

group mean. However, the average abundances are similar for each meteorite, and the group mean therefore shows a smaller nominal deviation. In most cases, elemental uncertainties in individual meteorites reflect true abundance variations within the given meteorite and not necessarily differences in analytical procedures and results.

The CI chondrite elemental concentrations by mass from Table 3 were divided by the respective atomic weights and normalized to  $\text{Si} = 10^6$  atoms to obtain the data on the cosmochemical abundance scale shown in column (5) of Table 1. For a comparison of the meteoritic with photospheric data, it is useful to place the meteoritic abundances on the astronomical log scale, which is normalized to  $A(\text{H}) = 12$ . However, CI chondrites are depleted in hydrogen, and therefore the meteoritic abundances are coupled to the astronomical scale using another element. Here the meteoritic abundances on the astronomical log scale are shown in column (6), and were calculated using the relationship

$$A(\text{El}) = 1.540 + \log N(\text{El}), \quad (2)$$

so that the Si abundance from the cosmochemical scale equals the photospheric Si abundance of  $A(\text{Si}) = 7.54$  on the astronomical scale. The value of 1.540 was selected to obtain an exact match of the Si abundance on both scales. This approach is the same as used by Suess & Urey (1956) in their seminal paper, but is somewhat different from that used in other compilations (e.g., Cameron 1973, 1982; Grevesse 1984; Anders & Grevesse 1989; Palme & Beer 1993), in which the scale-coupling factor was obtained by averaging differences of  $A(\text{El})_{\text{photo}} - \log N(\text{El})_{\text{CI}}$  of several elements from photospheric and meteoritic abundance determinations. For example, an individual scale-coupling factor can be calculated for 35 elements. The number of elements was limited here by the nominal uncertainties in the photospheric abundances, which must be below 25% in order to include an element in the comparison. (Note that this approach does not include all 41 elements for which the mean photospheric and meteoritic abundances agree within 15%, because it only relies on the quality of the photospheric abundance determinations.) This yields a coupling factor of  $1.539 \pm 0.046$ , not much different from the direct approach using silicon only. The approach of coupling the two scales by the use of an average factor is probably not necessary and seems to be a tradition from the past, when photospheric abundance determinations were more uncertain. There is also the question of which elements to include in obtaining such a coupling factor. Here the photospheric abundance uncertainty is used as a criterion, but someone else may choose different selection criteria. I prefer the direct coupling of the astronomical and cosmochemical scale for meteoritic abundance by silicon, which is already used to normalize the cosmochemical scale. This is much more straightforward and not associated with any bias in the selection of elements entering an average coupling factor. Also note that there is no need for a coupling factor at all if a comparison of meteoritic and photospheric abundances is done by using the cosmochemical abundance scale, because both abundance sets can *independently* be normalized to  $\text{Si} = 10^6$  atoms or another element that is well determined in both sets. However, often the comparison of meteoritic and photospheric abundances is only done using the logarithmic scale (e.g., Grevesse 1984; Anders & Grevesse 1989; Palme & Beer 1993; Grevesse & Sauval 1998). Comparisons

of the two elemental abundance sets both independently normalized to  $\text{Si} = 10^6$  atoms appears much more practical, because this avoids the logarithmic conversion factor altogether. In Table 1, meteoritic and photospheric abundances are given on both the astronomical and cosmochemical scales to facilitate comparisons.

### 2.3. Selection of Photospheric Abundances

The solar photospheric abundances serve as a reference for abundance determinations in other astronomical objects, and a reliable photospheric abundance set is desirable. The selected photospheric abundances from solar and meteoritic abundance determinations are given in columns (2) and (3) of Table 1. Column (4) indicates if the photospheric (“s”) or meteoritic (“m”) abundance is selected, and “a” indicates that the average of the solar and meteoritic abundances is adopted. The average is used either because both abundance determinations yield a similar value, or because photospheric and meteoritic values both have similar uncertainties, so that the uncertainty cannot serve as a guide to the “best” value. A “t” in column (4) indicates that a theoretical value was used.

The uncertainties listed in Table 1 for spectroscopic observations are those quoted in the references the values were taken from. The uncertainty for a given element in the CI chondrite abundances in Table 1 is the larger value of either the deviation of the weighted group mean from Table 3 or the maximum standard deviation for any of the individual meteorites. Thus, the uncertainties of CI chondritic abundances in Table 1 should reflect an upper limit to the variations in elemental abundance.

As mentioned above, the agreement between photospheric and meteoritic abundances is within 0.06 dex (15%) for 41 out of 56 rock-forming elements, and many values are indistinguishable within the uncertainties. Excluding Li, Be, and B (§ 2.3.2), large disagreements are found for rock-forming elements that have large uncertainties in photospheric abundance determinations (e.g., Au, Hf, In, Mn, Sn, Tm, W, Yb) and for elements whose abundances are also more variable in meteorites (e.g., Cl, Ga, Rb). These disagreements may be resolved when new transition probabilities become available and are applied to the photospheric abundance determinations. Most discrepant are W and In. The photospheric W abundance of  $A(\text{W}) = 1.11 \pm 0.15$  used here is from Grevesse (1984), which is based on the work by Holweger & Werner (1982). A new analysis of the faint W line on which the abundance is based is probably necessary (see Grevesse 1984). Recently, Bord & Cowley (2002) reanalyzed the photospheric In abundance, but as they discuss, the reason for the huge discrepancy between the meteoritic and photospheric In abundance remains elusive.

The abundances of Ti and Sc also deserve some brief comment, as they remain problematic despite the application of new transition probabilities to their photospheric determinations (Grevesse & Noels 1993). The photospheric Ti abundance  $A(\text{Ti}) = 5.02 \pm 0.06$  in Table 1 is the value recommended by Grevesse et al. (1996), somewhat lower than  $A(\text{Ti}) = 5.04 \pm 0.04$  from Bizzarri et al. (1993). These values are not significantly different from  $A(\text{Ti}) = 4.99 \pm 0.02$  from Grevesse, Blackwell, & Petford (1989). Thus, a difference of  $\sim 0.08$  dex between the photospheric and meteoritic abundance of  $A(\text{Ti}) = 4.92 \pm 0.03$  still needs



to be explained. Similarly, the photospheric Sc abundance of  $A(\text{Sc}) = 3.10 \pm 0.09$  adopted by Grevesse (1984) was changed to  $A(\text{Sc}) = 3.05 \pm 0.08$  by Youssef & Amer (1989), who used updated transition probabilities, as did Neuforge (1993), whose abundance of  $A(\text{Sc}) = 3.17 \pm 0.10$  was adopted by Grevesse & Noels (1993). Within the large uncertainty, the latter value just approaches the meteoritic abundance of  $A(\text{Sc}) = 3.07 \pm 0.04$ . The following sections describe the abundance selection of several other elements in more detail.

### 2.3.1. Elements Enriched in the Photosphere Relative to CI Chondrites: H, C, N, O, and Noble Gases

The selected photospheric abundances of H, C, N, O and the noble gases He, Ne, and Ar in Table 1 are those obtained from “solar” determinations, because these elements are not quantitatively retained in meteorites.

The photospheric abundances of oxygen and carbon were redetermined recently by Allende Prieto et al. (2001, 2002). Compared to the selected abundances of Grevesse & Sauval (1998) and Anders & Grevesse (1989), the carbon abundance is now smaller by a factor of 1.4 or 1.5, respectively, and the oxygen abundance is reduced by a factor 1.4 or 1.7. The selected nitrogen abundance is that from Holweger (2001), lowered by 0.1 dex as suggested by Allende Prieto et al. (2002).

The comparison of solar and meteoritic abundances given in Table 1 shows that C, N, O, and H are only partially incorporated into rocky material. The CI chondrites have about 50% of the photospheric oxygen, 10% of the photospheric carbon, and 3% of the photospheric nitrogen abundance. Compared to the photospheric abundance, very little hydrogen ( $\sim 0.02\%$  of total photospheric H) is found in hydrated minerals and organic matter in CI chondrites. The selection of photospheric abundances of He and other noble gases is described below.

#### 2.3.1.1. Helium Abundance

The helium abundance cannot be derived from the solar photospheric spectrum, so other methods must be employed. These methods provide He abundances for different times in the Sun’s evolution, and results are summarized in Table 4. The discussion of the He abundance is tied to the mass fractions of H, He, and the heavy elements, which are commonly designated as  $X$ ,  $Y$ , and  $Z$ , respectively, with  $X + Y + Z = 1$ . In the following, values without subscripts refer to current photospheric data and values with subscript “0” to protosolar data.

Anders & Grevesse (1989) derived the protosolar He content [ $A(\text{He})_0 = 10.99$ ] from H II regions and B stars of similar metallicity as the Sun. Heavy-element diffusion in the Sun was not considered, and it was assumed that element/hydrogen ratios of the photosphere were representative of the metallicity of the proto-Sun. In Table 4 this assumption is indicated by  $(Z/X)_0 \equiv (Z/X)_{\text{present}}$ . The protosolar value of  $A(\text{He})_0 = 10.99$  was also adopted in other compilations (Grevesse & Noels 1993; Grevesse et al. 1996) until the more recent He abundance determinations from solar standard models (SSM) and helioseismic data (see reviews by Christensen-Dalsgaard 1998, 2002) showed that the present He photospheric abundance is lower than  $A(\text{He}) = 10.99$ . This means that a combination of the protosolar He abundance of  $A(\text{He})_0 = 10.99$  with other current photospheric

elemental abundances returns neither the correct overall photospheric abundances nor the correct overall protosolar abundances.

Standard solar models describe the evolution and structure of the Sun to its present state from the protosolar composition. The initial mass fractions of H, He, and the heavy elements ( $X_0$ ,  $Y_0$ ,  $Z_0$ ) are one input to these models. The Sun’s interior structure depends on composition and is not uniform because of nuclear reactions and gravitational settling of helium and heavy elements, i.e.,  $Y < Y_0$  and  $Z < Z_0$ , so that  $X > X_0$ . The diffusion of He and heavy elements was formerly only included in the so-called “non-standard” solar models but now is integrated into most standard models. The helium mass fraction strongly influences the luminosity, and the amount of heavy elements is important because these elements serve as opacity sources. The test of solar models and their input parameters is whether or not they match the current radius, mass, and surface luminosity of the Sun, and the present composition ( $X$ ,  $Y$ ,  $Z$ ) of the photosphere. However, the mass fraction or abundance of He in the photosphere is uncertain and is left as a free parameter. Only the mass ratio of heavy elements to hydrogen ( $Z/X$ ), which is of course independent of  $Y$ , serves as a test parameter.

It has been argued that the current  $Z/X$  is well constrained and may rule out heavy-element settling, because meteoritic and photospheric abundances agree, but this argument is flawed. The mass fraction  $Z$  is mainly determined by the sum of the masses of the light elements C, N, O, Ne, and the major rock-forming elements such as Si, Mg, Fe, etc. Typically, C, N, O, and Ne make up more than half of the total mass included in  $Z$ . However, meteorites only provide information on the relative abundances of the rock-forming elements. For comparison with photospheric abundances, the meteoritic abundances are renormalized to match the Si abundances in the photosphere. After renormalization to the same scale, the relative abundances of rock-forming elements such as Fe/Si or Mg/Si agree for CI chondrites and the photosphere. Meteoritic abundances can be used only to define the *relative* contribution of rock-forming elements within  $Z$ , but not the absolute value of  $Z$  or the  $Z/X$  ratio. The mass fraction of hydrogen is not constrained by meteoritic abundances, and  $Z/X$  remains a solely photospheric quantity. The agreement of the relative abundances of rock-forming elements in the photosphere and in meteorites cannot be taken as an argument that heavy-element settling does not occur in the Sun. If all rock-forming elements settled from the photosphere by the same amount, the relative abundances of rock-forming elements in the photosphere would still be the same as in CI chondrites.

The standard solar models derive not only the present-day He abundance in the outer convective zone (taken as representative of the photosphere) but also the initial mass fractions of He ( $Y_0$ ) and heavy elements ( $Z_0$ ). When available, both present and protosolar values from individual SSMs are given in Table 4. The model described by Christensen-Dalsgaard (1998) yields an initial composition of  $Y_0 = 0.2713$ ,  $Z_0 = 0.0196$ ,  $X_0 = 0.7091$  (with  $Z_0/X_0 = 0.0276$ ), which satisfies the observed luminosity and radius of the present Sun and the observed photospheric  $Z/X$  ratio of  $0.0245 \pm 0.0025$  from Grevesse & Noels (1993) and Grevesse & Sauval (1998). Converting the initial He mass fraction ( $Y_0$ ) to the atomic scale yields  $A(\text{He})_0 = 10.98$  for the time of the Sun’s formation. One of the models by

TABLE 4  
HELIUM ABUNDANCE AND MASS FRACTIONS

$X$	$Y$	$Z$	$Z/X$	$n(\text{He})/n(\text{H})$	$A(\text{He})$	Timing	Notes	References
0.7068	0.2743	0.0189	0.0267	0.0970	10.99	Protosolar	He from H II regions, $(Z/X)_0 \equiv (Z/X)_{\text{present}}$	1
0.703	0.280	0.017	0.0245	0.100	11.0	Protosolar	$(Z/X)_0 \equiv (Z/X)_{\text{present}}$	2
0.7080	0.2747	0.0173	0.0244	0.098	10.99	Protosolar	$(Z/X)_0 \equiv (Z/X)_{\text{present}}$	3
0.7091	0.2713	0.0196	0.0276	0.096	10.98	Protosolar	SSM using $Z/X$ of reference 2 $(Z/X)_0 > (Z/X)_{\text{present}}$	4
0.7340	0.248	0.0180	0.0245	0.0851	10.93	Present	helioseismic data, $Z/X$ of reference 2	5,6
0.7352	0.248	0.0168	0.0229	0.0849	10.93	Present	He from helioseismic data from reference 6 who used $Z/X$ from reference 2	7
0.7367	0.248	0.0153	0.0208	0.0848	10.93	Present	He from helioseismic data from reference 6 who used $Z/X$ of reference 2	8
0.7046	0.2754	0.0200	0.0284	0.0984	10.993	Protosolar	SSM no. 3 of reference 9, using $Z/X$ of reference 2;	9
0.7369	0.2451	0.0180	0.0244	0.0838	10.923	Present	$(Z/X)_0 > (Z/X)_{\text{present}}$ SSM no. 3 of reference 9, using $Z/X$ of reference 2;	9
0.7037	0.2760	0.0203	0.0288	0.0987	10.995	Protosolar	$(Z/X)_0 > (Z/X)_{\text{present}}$	10
0.7395	0.2424	0.0181	0.0245	0.0825	10.917	Present	$(Z/X)_0 > (Z/X)_{\text{present}}$ SSM no. 1 in reference 10 using $Z/X$ of reference 2;	10
0.7081	0.2749	0.0170	0.0240	0.0978	10.990	Protosolar	$(Z/X)_0 > (Z/X)_{\text{present}}$ SSM no. 1 in reference 10 using $Z/X$ of reference 2;	10
0.7453	0.2396	0.0151	0.0203	0.0810	10.908	Present	$(Z/X)_0 > (Z/X)_{\text{present}}$ SSM no. 31 in reference 10 using $X/Z = 0.0203$ , $(Z/X)_0 > (Z/X)_{\text{present}}$	10
0.7110 $\pm$ 0.0040	0.2741 $\pm$ 0.0120	0.0149 $\pm$ 0.0015	0.0210 $\pm$ 0.0021	0.0964 $\pm$ 0.0043	10.984 $\pm$ 0.019	Protosolar	$(Z/X)_0 > (Z/X)_{\text{present}}$	11
0.7491 $\pm$ 0.0030	0.2377 $\pm$ 0.0030	0.0133 $\pm$ 0.0014	0.0177 $\pm$ 0.0018	0.0793 $\pm$ 0.0010	10.899 $\pm$ 0.005	Present	$(Z/X)_0 > (Z/X)_{\text{present}}$	11

NOTE.—SSM: standard solar model.  $(Z/X)_0 \equiv (Z/X)_{\text{present}}$  means heavy-element and He diffusion is not taken into account.  $(Z/X)_0 > (Z/X)_{\text{present}}$  means heavy-element and He diffusion is taken into account.

REFERENCES—(1) Anders & Grevesse 1989; (2) Grevesse & Noels 1993; (3) Grevesse et al. 1996; (4) Christensen-Dalsgaard 1998; (5) Richard et al. 1998; (6) Dziembowski 1998; (7) Grevesse & Sauval 1998; (8) Grevesse & Sauval 2002; (9) Gabriel 1997; (10) Boothroyd & Sackmann 2003; (11) this work.

Gabriel (1997) taking diffusion into account also returns the observed  $Z/X$  ratio of 0.0245 adopted at that time. The corresponding helium mass fraction yields a current He abundance of  $A(\text{He}) = 10.92$ , and the initial He mass fraction gives a protosolar helium abundance of  $A(\text{He})_0 = 10.99$ . A recent detailed study by Boothroyd & Sackmann (2003) gives essentially the same results.

Many of the recent solar models (e.g., Christensen-Dalsgaard 1998; Boothroyd & Sackmann 2003) are calibrated to the observed  $Z/X$  ratio from the abundance table by Grevesse & Noels (1993), mainly because opacity tables are available for this composition. Helioseismic models used for comparison with SSMs also use the Grevesse & Noels (1993) data. However, since Grevesse (1984), the  $Z/X$  ratio has dropped because abundances of the major heavy elements (C, N, O, Ne), although associated with large uncertainties, are steadily revised downward. This trend is summarized in Table 5. Because the more recent  $Z/X$  ratios are lower, it is not appropriate to directly adopt the He abundances from SSMs calibrated for  $Z/X = 0.0245$ . A lower photospheric  $Z/X$  implies a correspondingly lower  $Z_0/X_0$  as well as lower  $Y$  and  $Y_0$  values from SSMs because opacity from heavy elements is reduced and a lower initial He abundance may suffice in matching the solar luminosity.

The selected photospheric abundances here from Table 1 give  $Z/X = 0.0177$ , which is only about three-quarters of the  $Z/X = 0.0245$  used in many SSM and helioseismic models. In the absence of detailed SSMs calibrated for the photospheric  $Z/X$  ratio adopted here, the following approach is used to find the He abundance.

Boothroyd & Sackmann (2003) present a comprehensive study of how input parameters affect solar modeling. The results from their reference model (model 1 in their paper) and models with lower  $Z/X$  ratios (their models 29–31) are used to derive scaling relations for an estimate of the helium mass fraction. The results from their model with the lowest  $Z/X$  ratio that still satisfies observed solar data are shown for comparison in Table 4. A fit for the data of models 1 and 29–31 of Boothroyd & Sackmann (2003) gives  $Y = 0.2246(\pm 0.0019) + 0.7409(\pm 0.0818)(Z/X)$ . This yields  $Y = 0.2377(\pm 0.0030)$  for  $Z/X = 0.0177$  selected here. The uncertainty in  $Y$  includes the uncertainty from the fit parameters and a 10% uncertainty in  $Z/X$ , which enters  $Z$  from uncertainties in the C, N, O, and Ne abundances (Table 1).

TABLE 5  
PHOTOSPHERIC  $Z/X$  IN ELEMENTAL  
ABUNDANCE COMPILATIONS

$Z/X$	Year	Reference
0.0270 .....	1984	1
0.0267 .....	1989	2
0.0245 .....	1993	3
0.0244 .....	1996	4
0.0229 .....	1998	5
0.0208 .....	2002	6
0.0177 .....	2003	7

REFERENCES—(1) Grevesse 1984; (2) Anders & Grevesse 1989; (3) Grevesse & Noels 1993; (4) Grevesse et al. 1996; (5) Grevesse & Sauval 1998; (6) Grevesse & Sauval 2002; (7) this work.

In order to convert the helium mass fraction to the atomic He abundance, the mass fraction of hydrogen ( $X$ ) or the mass fraction ratio  $Y/X$  must be computed. The absolute mass fractions of hydrogen and heavy elements are uniquely defined for a given ( $Z/X$ ) and the corresponding helium mass fraction by the equations

$$X = \frac{1 - Y}{1 + (Z/X)}, \quad Z = 1 - X - Y. \quad (3)$$

The atomic  $n(\text{He})/n(\text{H})$  ratio and the He abundance [ $A(\text{He})$ ] on the atomic scale depend on  $Y$  and  $Z/X$  because

$$\frac{n(\text{He})}{n(\text{H})} = \frac{Y}{4X} = \frac{Y(1 + Z/X)}{4(1 - Y)}. \quad (4)$$

Inserting the values for  $Y$  and  $Z/X$  obtained here gives  $n(\text{He})/n(\text{H}) = 0.0793(\pm 0.0010)$  and a photospheric helium abundance of  $A(\text{He}) = 10.899 \pm 0.005$ . The uncertainty in  $A(\text{He})$  includes that from the fit and those in  $X$ ,  $Y$ , and  $Z$  (see Table 4).

It is convenient to also describe the derivation of the protosolar He abundance (§ 2.4) in this section. Again, scaling relations from the models by Boothroyd & Sackmann (2003) are used. The present and protosolar  $Z/X$  ratios in the models mentioned above give the correlation  $(Z_0/X_0) = 6.545(\pm 0.937) \times 10^{-4} + 1.150(\pm 0.004)(Z/X)$ , which is used to obtain  $Z_0/X_0 = 0.0210 \pm 0.0021$  from the photospheric  $Z/X$  ratio above. As the uncertainties in the fit parameters are small, the uncertainty in  $Z_0/X_0$  is essentially the same (10%) as for  $Z/X$ .

The protosolar helium mass fraction is estimated from Boothroyd & Sackmann's data by relating  $Y_0$  to  $Y$  with the fit  $Y_0 = 0.1685(\pm 0.009) + 0.4441(\pm 0.0357)Y$ . This yields the protosolar  $Y_0 = 0.2741 \pm 0.0120$ . The absolute mass fractions  $X_0$  and  $Z_0$  are then obtained from equation (3), and the helium abundance is calculated by inserting  $Y_0$  and  $Z_0/X_0$  into equation (4). The protosolar helium abundance is  $A(\text{He})_0 = 10.984 \pm 0.019$ , where the uncertainty includes all uncertainties from the fit parameters and 10% uncertainty in the photospheric  $Z/X$  ratio.

### 2.3.1.2. Neon Abundance

The Ne and Ar abundances are often derived from solar wind (SW), solar energetic particles (SEP), and impulse flare spectra (see, e.g., Grevesse & Noels 1993; Meyer 1989, 1996). Holweger (2001) evaluated the Ne abundance as  $A(\text{Ne}) = 8.001 \pm 0.069$  using Ne/Mg and O/Ne ratios from extreme-ultraviolet (EUV) observations of emerging active regions as given by Widing (1997). Using the same procedure as described by Holweger (2001), the adopted oxygen abundance (Allende Prieto et al. 2001), and Mg abundance (Holweger 2001), I obtain a Ne abundance of  $7.99 \pm 0.07$ , slightly lower than Holweger's value. However, this approach assumes that the O/Mg ratio is photospheric in the emerging regions. Widing's O/Mg ratio is  $21.6 \pm 2.1$ , which appears to be close to the photospheric value of O/Mg = 22.2 from Anders & Grevesse (1989) or 19.5 from Grevesse et al. (1996). The O/Mg ratio from the selected photospheric data here is 13.9; the selected data by Holweger (2001) also give a lower O/Mg ratio of 15.8. This could indicate fractionations related to the first ionization potential (FIP) effect in the emerging regions observed by Widing (1997), because Mg is a low-FIP element, while O



and Ne are high-FIP elements. A more conventional procedure to obtain the neon abundance is to use the Ne/O ratio only, because the FIP effect is more likely to cancel out. The Ne/O ratio appears more constant in different environments. Meyer (1989) reviewed Ne and O abundances in hot stars and Galactic H II regions and found  $\text{Ne/O} = 0.155 \pm 0.035$ ; SEP data by Reames (1998) show  $\text{Ne/O} = 0.152 \pm 0.004$ ; and Widing (1997) found  $\text{Ne/O} = 0.150 \pm 0.02$  in the emerging regions. The average from all these data is  $0.152 \pm 0.041$ , which combined with the selected photospheric oxygen abundance gives  $A(\text{Ne}) = 7.87 \pm 0.10$ . This adopted photospheric Ne abundance is 0.2 dex lower than the Ne abundance given by Grevesse & Sauval (1998). Interestingly, Del Zanna, Bromage, & Mason (2003) find that coronal plumes have photospheric abundances, except for Ne, for which they derived an abundance 0.2 dex below the photospheric value given by Grevesse & Sauval (1998). However, with the lower Ne abundance obtained here, the discrepancy between the photospheric and coronal plume data is removed.

### 2.3.1.3. Argon Abundance

Young et al. (1997) re-evaluated the photospheric Ar abundance as  $6.47 \pm 0.10$ , based mainly on the Ar/O ratio of the solar wind as observed in lunar soils. They re-evaluated Ar in order to compare the photospheric Ar/Ca ratio to their Ar/Ca measurements of coronal plasma, where Ar and Ca are fractionated as a result of the FIP effect (which means that Ar/Ca from coronal plasma cannot be used to derive the photospheric Ar abundance). Grevesse & Sauval (1998) compared the photospheric Ar data of Young et al. (1997) to the SEP abundance of Ar from Reames (1998) and selected the latter as  $A(\text{Ar}) = 6.40 \pm 0.06$  because of the smaller uncertainty. However, Ar is a high-FIP element like C, N, O, and Ne, so Ar should be depleted in SEPs relative to the photosphere as are the other high-FIP elements (see Fig. 2 of Reames 1998). Hence, the SEP value of  $A(\text{Ar}) = 6.39 \pm 0.026$  listed by Reames (1998) only represents a lower limit to the actual photospheric Ar abundance, as does the value from Young et al. (1997) derived from solar wind data for similar reasons. Both values are much smaller than the value  $A(\text{Ar}) = 6.56 \pm 0.10$  given by Anders & Grevesse (1989), who also considered SW and SEP data for photospheric Ar, but not before adding a factor correcting for coronal/photospheric fractionations.

The Ar abundance selected here is from an interpolation of the  $^{36}\text{Ar}$  abundance between  $^{28}\text{Si}$  and  $^{40}\text{Ca}$ , where local nuclear statistical equilibrium is well-established (Cameron 1973, 1982). The  $^{36}\text{Ar}$  abundance derived from this semi-equilibrium abundance method is then scaled to the elemental photospheric Ar abundance of  $A(\text{Ar}) = 6.55 \pm 0.08$  using the isotopic abundances listed in Table 6. This abundance is assigned an uncertainty of 20%.

### 2.3.1.4. Krypton and Xenon Abundances

The abundances of the heavy noble gases Kr and Xe are based on theoretical values from neutron-capture element systematics, renormalized to the selected Si abundance here. The Kr abundance  $A(\text{Kr}) = 3.28 \pm 0.08$  is from the data given by Palme & Beer (1993), who considered contributions from the main and weak *s*-process to the  $^{82}\text{Kr}$  isotopic composition, which was then combined with the abundances of the Kr isotopes from Wieler (2002; see Table 6) to

obtain the Kr elemental abundance. This Kr abundance is about 13% higher than  $A(\text{Kr}) = 3.23 \pm 0.07$  from Anders & Grevesse (1989). In this respect, it is worth mentioning that Raiteri et al. (1993) also concluded that the solar elemental Kr abundance from Anders & Grevesse (1989) was underestimated by 20%.

For Xe, Palme & Beer (1993) derive  $A(\text{Xe}) = 2.16 \pm 0.09$ , about 15% lower than  $A(\text{Xe}) = 2.23 \pm 0.08$  selected by Anders & Grevesse (1989). More recently, Reifarth et al. (2002) measured new neutron cross sections for important Xe process nuclei. They derive  $N(\text{Xe}) = 5.39 \pm 0.22$ , or  $A(\text{Xe}) = 2.27 \pm 0.02$ , using neutron-capture systematics on  $^{130}\text{Xe}$  and the isotopic abundances of the Xe isotopes from Anders & Grevesse (1989). This Xe abundance is not changed if the isotopic abundances from Wieler (2002) are applied, although there are minor changes in the absolute abundance of the individual Xe isotopes (see Table 6). The elemental Xe abundance is 10%–20% higher than in the previous computations, and the level of uncertainty dropped significantly.

### 2.3.1.5. Noble Gases in CI Chondrites

The noble gas abundances thought to be indigenous to CI chondrites are given for comparison in Table 1. These abundances were obtained by scaling the isotopic abundances (in  $\text{nl g}^{-1}$  or  $\text{pl g}^{-1}$ ) of  $^4\text{He}$ ,  $^{20}\text{Ne}$ ,  $^{36}\text{Ar}$ ,  $^{84}\text{Kr}$ , and  $^{132}\text{Xe}$  given by Anders & Grevesse (1989) to elemental abundances, taking the isotopic contribution to each element into account. When compared to the selected photospheric abundances, the noble gas abundances in CI chondrites follow a depletion trend correlated with their atomic masses, with Xe depleted by a factor of  $\sim 10^4$  and Ne depleted by a factor of  $\sim 10^9$ . Obviously, the meteoritic noble gas abundances cannot be used to refine photospheric abundances.

### 2.3.2. Elements Depleted in the Sun Relative to CI Chondrites: Li, Be, and B

Until recently, the light elements Li, B, and Be were thought to be depleted in the Sun. However, new analyses of B and Be in the photosphere and in CI chondrites suggest that B and Be are apparently not destroyed in the Sun, leaving a problem for theorists to explain why only Li is processed, but not Be and B (see, e.g., Grevesse & Sauval 1998). The abundance determinations of Li in the Sun and in CI chondrites are relatively certain and show that the photospheric Li abundance is about 150 times lower than the value preserved in meteorites. However, abundance determinations of B and Be are problematic in both the Sun and meteorites, as described next.

#### 2.3.2.1. Beryllium Abundance

The photospheric Be abundance of  $A(\text{Be}) = 1.15 \pm 0.20$  from Chiemlewski, Müller, & Brault (1975) served as the solar reference value until Balachandran & Bell (1998) revised the abundance to  $A(\text{Be}) = 1.40 \pm 0.09$ . Within uncertainties, the latter photospheric abundance is in agreement with the meteoritic Be abundance of 1.42 from Anders & Grevesse (1989) or the  $1.41 \pm 0.08$  selected here (Table 1). This agreement suggests that the Sun is not depleted in Be. However, both the photospheric and the meteoritic abundance determinations are uncertain.

Balachandran & Bell (1998) suggested that UV opacity in the regions of the accessible Be II lines had to be increased,

TABLE 6  
ABUNDANCES OF THE ISOTOPES IN THE SOLAR SYSTEM

Element	<i>A</i>	Atom %	Abundance	Element	<i>A</i>	Atom %	Abundance	Element	<i>A</i>	Atom %	Abundance	
1 H.....	1	99.99806	$2.431 \times 10^{10}$	21 Sc.....	45	100	34.20	37 Rb.....	85	72.1654	4.743	
	2	0.00194	$4.716 \times 10^5$		22 Ti.....	46	8.249		200	87	27.8346	1.829
		100	$2.431 \times 10^{10}$			47	7.437		180		87*	
2 He.....	3	0.016597	$3.889 \times 10^5$	48		73.72	1785		100			6.572
	4	99.983403	$2.343 \times 10^9$	49	5.409	131	38 Sr.....	84	0.5551	0.13124		
	100	$2.343 \times 10^9$	3 Li.....	50	5.185	126		86	9.8168	2.32069		
6	7.589	4.21		23 V.....	50	0.2497	0.720	87	7.3771	1.7439		
7	92.411	51.26	51		99.7503	287.68	87*		1.62181			
	100	55.47	100		288.4	39 Y.....		89	100	4.608		
4 Be.....	9	100	0.7374	24 Cr.....	50		4.3452	559	40 Zr.....	90	51.452	5.830
5 B.....	10	19.82	3.433		52	83.7895	10775	91		11.223	1.272	
	11	80.18	13.887		53	9.5006	1222	92		17.146	1.943	
	100	17.32	6 C.....		54	2.3647	304	94		17.38	1.969	
12	98.8922	$7.001 \times 10^6$		100	12860	25 Mn.....	55	100	9168			
13	1.1078	78420	100	7.079 $\times 10^6$	54		5.845	48980	41 Nb.....	93	100	0.7554
7 N.....	14	99.6337	$1.943 \times 10^6$	26 Fe.....	56	91.754	768,900	42 Mo.....		92	14.8362	0.386
	15	0.3663	7143		57	2.119	17760		94	9.2466	0.241	
		100	$1.950 \times 10^6$		58	0.282	2360		95	15.9201	0.414	
8 O.....	16	99.7628	$1.410 \times 10^7$	27 Co.....	59	100	2323	96	16.6756	0.434		
	17	0.0372	5260		28 Ni.....	58	68.0769	32541	97	9.5551	0.249	
	18	0.20004	28270			60	26.2231	12532	98	24.1329	0.628	
	100	$1.413 \times 10^7$	61	1.1399		545	100	9.6335	0.251			
9 F.....	19	100	841.1	62	3.6345	1737	44 Ru.....	96	5.542	0.1053		
10 Ne.....	20	92.9431	$1.996 \times 10^6$	64	0.9256	442		98	1.8688	0.0355		
	21	0.2228	4786	100	47800	29 Cu.....	99	12.7579	0.242			
	22	6.8341	$1.468 \times 10^5$	63	69.174		364.5	100	12.5985	0.239		
	100	$2.148 \times 10^6$	65	30.826	162.5		101	17.06	0.324			
11 Na.....	23	100	57510	100	527.0	30 Zn.....	102	31.5519	0.599			
12 Mg.....	24	78.992	$8.057 \times 10^5$	64	48.63		596	104	18.621	0.354		
	25	10.003	$1.020 \times 10^5$	66	27.9		342	100	1.900			
	26	11.005	$1.123 \times 10^5$	67	4.10	50.3	45 Rh.....	103	100	0.3708		
	100	$1.020 \times 10^6$	68	18.75	230	46 Pd.....		102	1.02	0.0146		
13 Al.....	27	100	84100	70	0.62			7.6	104	11.14	0.160	
14 Si.....	28	92.22968	$9.2230 \times 10^5$	100	1226		31 Ga.....	69	60.1079	21.62		
	29	4.68316	46830	71	39.8921	14.35		70	0.62	7.6		
	30	3.08716	30870	100	1226	32 Ge.....		70	21.234	25.6		
	100	$1.000 \times 10^6$	72	27.662	33.4		72	27.662	33.4			
15 P.....	31	100	8373	73	7.717		9.3	73	7.717	9.3		
16 S.....	32	95.018	$4.227 \times 10^5$	74	35.943	43.3	74	35.943	43.3			
	33	0.75	3340	76	7.444	9.0	76	7.444	9.0			
	34	4.215	18750	100	120.6	33 As.....	75	100	6.089			
	36	0.017	76	70	21.234		25.6	74	0.889	0.58		
	100	$4.449 \times 10^5$	72	27.662	33.4		76	9.366	6.16			
17 Cl.....	35	75.771	3968	73	7.717	9.3	77	7.635	5.02			
	37	24.229	1269	74	35.943	43.3	78	23.772	15.64			
		100	5237	76	7.444	9.0	80	49.607	32.64			
18 Ar.....	36	84.5946	86710	82	8.731	5.74	34 Se.....	74	0.889	0.58		
	38	15.3808	15765	100	65.79	35 Br.....		76	9.366	6.16		
	40	0.0246	25	79	50.686			5.74	77	7.635	5.02	
	40		24	81	49.314	5.58	78	23.772	15.64			
		100	102,500	100	11.32	36 Kr.....	78	0.362	0.20			
19 K.....	39	93.25811	3443	80	2.33		1.28	80	2.33	1.28		
	40	0.011672	0.431	82	11.65		6.43	82	11.65	6.43		
	40*		5.37	83	11.55	6.37	83	11.55	6.37			
	41	6.73022	248.5	84	56.90	31.38	84	56.90	31.38			
		100	3692	86	17.21	9.49	86	17.21	9.49			
20 Ca.....	40	96.941	60947	100	55.15	47 Ag.....	107	51.8392	0.2547			
	42	0.647	407	48 Cd.....	106		1.25	0.01980				
	43	0.135	84.9		108		0.89	0.01410				
	44	2.086	1311		110		12.49	0.198				
	46	0.004	2.5		111		12.8	0.203				
	48	0.187	118		112		24.13	0.382				
		100	62870		113		12.22	0.194				
			114		28.73	0.455						
			116	7.49	0.119							
			100	1.584	49 In.....	113	4.288	0.0078				
			100	55.15		115	95.712	0.173				
					100	0.181						



TABLE 6—Continued

Element	<i>A</i>	Atom %	Abundance	Element	<i>A</i>	Atom %	Abundance	Element	<i>A</i>	Atom %	Abundance
50 Sn .....	112	0.971	0.03625		150	5.62	0.04695	73 Ta .....	180	0.0123	0.0000258
	114	0.659	0.02460		100		0.8355		181	99.9877	0.020987
	115	0.339	0.01265	62 Sm .....	144	3.0734	0.00781		100		0.02099
	116	14.536	0.5426		147	14.9934	0.03811	74 W .....	180	0.1198	0.000153
	117	7.676	0.2865		147*		0.03926		182	26.4985	0.03384
	118	24.223	0.9042		148	11.2406	0.0286		183	14.3136	0.01828
	119	8.585	0.3205		149	13.8189	0.0351		184	30.6422	0.03913
	120	32.593	1.2167		150	7.3796	0.0188		186	28.4259	0.03630
	122	4.629	0.1728		152	26.7421	0.0680		100		0.1277
	124	5.789	0.2161		154	22.752	0.0578	75 Re .....	185	37.398	0.01965
	100		3.733		100		0.2542		187	62.602	0.03289
51 Sb .....	121	57.213	0.1883	63 Eu .....	151	47.81	0.04548		187*		0.03544
	123	42.787	0.1409		153	52.19	0.04965		100		0.05254
	100		0.3292		100		0.09513	76 Os .....	184	0.0198	0.000133
52 Te .....	120	0.096	0.0046	64 Gd .....	152	0.2029	0.00067		186	1.5922	0.010728
	122	2.603	0.1253		154	2.1809	0.00724		186*		0.010727
	123	0.908	0.0437		155	14.7998	0.04915		187	1.644	0.011080
	124	4.816	0.2319		156	20.4664	0.06797		187*		0.008532
	125	7.139	0.3437		157	15.6518	0.05198		188	13.2865	0.089524
	126	18.952	0.9125		158	24.8347	0.08248		189	16.1992	0.10915
	128	31.687	1.526		160	21.8635	0.07261		190	26.3438	0.17750
	130	33.799	1.627		100		0.3321		192	40.9142	0.27568
	100		4.815	65 Tb .....	159	100	0.05907		100		0.6738
53 I .....	127	100	0.9975	66 Dy .....	156	0.056	0.000216	77 Ir .....	191	37.272	0.2403
54 Xe .....	124	0.129	0.00694		158	0.096	0.000371		193	62.728	0.4045
	126	0.112	0.00602		160	2.34	0.00904		100		0.6448
	128	2.23	0.120		161	18.91	0.0730	78 Pt .....	190	0.013634	0.000185
	129	27.46	1.480		162	25.51	0.0985		190*		0.000186
	130	4.38	0.236		163	24.9	0.0962		192	0.78266	0.01062
	131	21.80	1.175		164	28.19	0.1089		194	32.967	0.44736
	132	26.36	1.421		100		0.3862		195	33.83156	0.45909
	134	9.66	0.521	67 Ho .....	165	100	0.08986		196	25.24166	0.34253
	136	7.87	0.424	68 Er .....	162	0.137	0.000350		198	7.16349	0.09721
	100		5.391		164	1.609	0.004109		100		1.357
55 Cs .....	133	100	0.3671		166	33.61	0.08584	79 Au .....	197	100	0.1955
56 Ba .....	130	0.1058	0.00460		167	22.93	0.05856	80 Hg .....	196	0.15344	0.00063
	132	0.1012	0.00440		168	26.79	0.06842		198	9.968	0.0411
	134	2.417	0.1052		170	14.93	0.03813		199	16.873	0.0697
	135	6.592	0.2868		100		0.2554		200	23.096	0.0953
	136	7.853	0.3417	69 Tm .....	169	100	0.0370		201	13.181	0.0544
	137	11.232	0.4887	70 Yb .....	168	0.13	0.000323		202	29.863	0.1233
	138	71.699	3.120		170	3.04	0.007551		204	6.865	0.0283
	100		4.351		171	14.28	0.03547		100		0.4128
57 La .....	138	0.09017	0.000397		172	21.83	0.05423	81 Tl .....	203	29.524	0.0545
	138*		0.000401		173	16.13	0.04007		205	70.476	0.1300
	139	99.90983	0.4401		174	31.83	0.07907		100		0.1845
	100		0.4405		176	12.76	0.03170	82 Pb .....	204	1.9820	0.064573
58 Ce .....	136	0.186	0.00217		100		0.2484		206	18.7351	0.61039
	138	0.251	0.00293	71 Lu .....	175	97.416	0.03480		206*		0.60091
	138*		0.00293		176	2.584	0.000923		207	22.5900	0.67082
	140	88.449	1.0340		176*		0.001008		207*		0.66497
	142	11.114	0.1299		100		0.03572		208	58.6929	1.91222
	100		1.169	72 Hf .....	174	0.1620	0.000275		208*		1.90335
59 Pr .....	141	100	0.1737		176	5.2502	0.0089201		100		3.258
60 Nd .....	142	27.16	0.22689		176*		0.0088353	83 Bi .....	209	100	0.1388
	143	12.19	0.1018631		177	18.5973	0.0315968		232	100	0.03512
	143*		0.1007121		178	27.2840	0.046356	90 Th .....	232*		0.04399
	144	23.83	0.1990728		179	13.6225	0.023145		235	0.72	0.000067
	145	8.30	0.06934		180	35.0840	0.059608	92 U .....	235*		0.005918
	146	17.17	0.14344		100		0.1699		238	99.2745	0.009238
	148	5.74	0.04795						238*		0.018713
									100		0.009306

NOTE.—Abundances on a scale where Si  $\equiv 10^6$ . Calculated for solar system abundances from Table 2 using mainly terrestrial isotopic compositions of Rosman & Taylor 1998, except for H and noble gases (see text). Values marked with asterisks are 4.55 Gyr ago. The 100% totals refer to present-day abundances.

which led to a higher solar Be abundance. This approach was recently questioned by Boesgaard et al. (2001), who argue in favor of the older solar Be abundance determined by Chiemiowski et al. (1975). Another problem with the Be abundance determination could be related to the oxygen abundance. One reason that Balachandran & Bell (1998) increased the UV opacity was the need to match the oxygen abundance from solar UV OH bands to that determined from IR bands of OH. Using the standard continuum opacity and the IR-based O abundance of  $A(O) = 8.75$ , Balachandran & Bell (1998) calculated UV OH features stronger than observed. Hence, they adopted a 1.6 times stronger continuum opacity for modeling. The oxygen abundance used by Balachandran & Bell (1998) is about 1.2 times larger than the new oxygen abundance of  $A(O) = 8.69$  determined by Allende Prieto et al. (2001). If the O abundance is lower, there may be no need to increase continuum opacity to match the UV OH features. In that case, the higher O abundance used by Balachandran & Bell (1998), and not the continuum opacity, could be the root of the problem, thus leading to an overestimate of the solar Be abundance. Until this issue is resolved, the photospheric Be abundance of Chiemiowski et al. (1975) is selected here.

The CI chondritic Be abundance is plagued with uncertainties stemming from the procedure used to obtain the value. Commonly, the CI chondritic Be abundance is derived indirectly by comparing refractory element abundance ratios among different carbonaceous chondrite groups (see, e.g., Anders & Grevesse 1989). This is done because only a single measurement of Be (19 ppb by mass) in one CI chondrite (Orgueil) is reported in the literature, in an abstract by Vilcsek (1977). This value is equivalent to a Be atomic abundance of  $A(Be) = 1.29$ . It is unclear whether or not this single determination is representative for CI chondrites because it is lower than expected from refractory element abundance systematics.

Beryllium is a refractory element like Ca and Al, and abundances of these and other refractory elements have been determined in carbonaceous chondrites of type CV and CM. The abundance ratios of refractory elements in CM (and CV) chondrites relative to CI chondrites yield approximately constant factors, e.g.,  $CM/CI = 1.40$  and  $CV/CI = 2.00$ . Mean Be abundances in CM and CV chondrites are  $34.5 \pm 5.7$  ppb and  $51.3 \pm 5.1$  ppb, respectively. The CM and CV chondrite abundances and enrichment factors give CI chondritic Be concentrations of  $24.6 \pm 4.1$  ppb (from CM) and  $25.7 \pm 2.6$  ppb (from CV). The average of these two values  $25.2 \pm 5$  ppb is adopted here, which leads to the CI chondrite abundance of  $A(Be) = 1.41 \pm 0.08$ . This method appears straightforward, but Be concentrations in CM and CV chondrites are only based on a few determinations. The value for CM chondrites is the average from two meteorites (Murchison and Murray) from analyses by Eisentraut, Griest, & Sievers (1971), Quandt & Herr (1974), Sill & Willis (1962), and Vilcsek (1977). The Be concentration for CV chondrites is based on three analyses from the Allende meteorite taken from Eisentraut et al. (1971), Quandt & Herr (1974), and Vilcsek (1977); there are no other published Be analyses for other CV chondrites.

The indirectly derived CI chondritic value,  $A(Be) = 1.41 \pm 0.08$ , is adopted here as the meteoritic abundance. When compared to the photospheric abundance of  $A(Be) = 1.15 \pm 0.20$  by Chiemiowski et al. (1975), the meteoritic value suggests that the Sun is depleted in Be by a

factor of  $\sim 1.8$ . The photospheric abundance  $A(Be) = 1.40 \pm 0.09$  from Balachandran & Bell (1998) is essentially the same as the meteoritic value, suggesting no Be depletion in the Sun. If one prefers the single direct CI chondrite Be abundance of  $A(Be) = 1.29$  and the photospheric value from Chiemiowski et al. (1975), the meteoritic value is still higher by a factor of  $\sim 1.4$ . However, if the single direct meteoritic Be determination is compared to the photospheric value from Balachandran & Bell (1998) the problem is further compounded because then the Sun, and not the meteorites, would be enriched by a factor of  $\sim 1.3$ . Currently, firm statements about the Be depletion, if any, in the Sun cannot be made, as the available data accommodate a range of depletion factors from 1 to 2 times lower than the meteoritic value. This issue can only be cleared up when problems in solar Be abundance determinations are resolved and more analyses of Be in CI chondrites are published.

### 2.3.2.2. Boron Abundance

The solar B abundance of  $A(B) = 2.7^{+0.21}_{-0.12}$  determined by Cunha & Smith (1999) is  $\sim 25\%$  larger than the previous value of  $A(B) = 2.6$  given by Kiselman & Carlsson (1996) and Kohl, Parkinson, & Withbroe (1977). Any of these values is lower than the meteoritic abundance of  $A(B) = 2.88 \pm 0.04$  selected by Anders & Grevesse (1989). While the solar B abundance was revised upward by 0.1 dex by Cunha & Smith (1999), the meteoritic B abundance has dropped by the same amount since Anders & Grevesse (1989). Boron analyses in meteorites are often unreliable because samples are easily contaminated. However, new analyses from interior samples of two CI chondrites by Zhai & Shaw (1994) yield a mean B concentration of  $0.71 \pm 0.07$  ppm (see Table 3), which translates to  $A(B) = 2.78 \pm 0.04$ . Taking the selected meteoritic and solar abundances at face value, B is slightly depleted in the Sun by a factor of  $\sim 1.2$ , but considering uncertainties in the photospheric and meteoritic values, this depletion may not be real.

### 2.3.3. Phosphorus Abundance

The photospheric P abundance of  $A(P) = 5.49 \pm 0.04$  determined by Berzonsh, Svanberg, & Biémont (1997) updates the previous value of  $A(P) = 5.45$  determined by both Biémont et al. (1994) and Lambert & Luck (1978). The latter value was selected for the solar abundance by Anders & Grevesse (1989) and Grevesse & Sauval (1998), and is smaller than their adopted meteoritic value of  $A(P) = 5.57$ . Recently, Wolf & Palme (2001) reanalyzed P in CI chondrites. Their results decrease the meteoritic abundance to  $A(P) = 5.43 \pm 0.05$  (Table 1). The new meteoritic P abundance is much closer to the older solar value of 5.45 than the new solar value of 5.49 from Berzonsh et al. (1997). However, the meteoritic value is only based on the P abundance in the Orgueil meteorite, for which a concentration of  $920 \pm 100$  ppm is derived (mainly from data by Wolf & Palme 2001). The P abundances of other CI chondrites are much more uncertain; for Ivuna, one reliable P analysis of 760 ppm exists (Wolf & Palme 2001), whereas P analyses of other CI chondrites date back several decades to almost a century, and range from 500 to 1800 ppm (see Mason 1963). Because both the photospheric and meteoritic abundances have 10% relative uncertainty, the average of

$A(P) = 5.46 \pm 0.04$  is adopted as representative for the solar photosphere.

#### 2.3.4. Sulfur Abundance

Grevesse (1984) adopted  $A(S) = 7.21 \pm 0.06$  for the photospheric S abundance, which was the widely used value until the recent determination of  $A(S) = 7.33 \pm 0.11$  by Biéumont, Quinet, & Zeppen (1993), which was adopted by Grevesse et al. (1996) and Grevesse & Sauval (1998). However, this sulfur abundance seems high compared to the meteoritic abundance (see following), and recent determinations of the photospheric abundance of  $A(S) = 7.20 \pm 0.03$  by Chen et al. (2002) and  $A(S) = 7.22 \pm 0.07$  by Takeda-Hirai et al. (2002) essentially reproduce the S abundance of  $A(S) = 7.23$  from Lambert & Luck (1978) and the selected photospheric value of  $A(S) = 7.21 \pm 0.06$  from Grevesse (1984). Here a photospheric  $A(S) = 7.21 \pm 0.05$  is selected from the most recent data.

The meteoritic value found by Anders & Grevesse (1989) is  $A(S) = 7.27 \pm 0.02$  based on five analyses of four CI chondrites given by Mason (1963). Palme & Beer (1993) recommend a meteoritic  $A(S) = 7.18 \pm 0.04$ , which is based on the average of 5.25% S by mass for the two Orgueil analyses given in Mason's (1963) compilation. The CI chondrite group-mean concentration of  $5.41 \pm 0.37\%$  by mass adopted here is the weighted average of the sulfur content of three CI chondrites for which S analyses are given by Curtis & Gladney (1985), Dreibus et al. (1995), Folinsbee, Douglas, & Maxwell (1967), Fredriksson & Kerridge (1988), and Mason (1963). This yields  $A(S) = 7.19 \pm 0.04$  for the meteoritic S abundance, which is chosen as representative for the photosphere because of the smaller uncertainty than that of the direct spectroscopic determination.

#### 2.3.5. Bromine and Iodine Abundances

There are no spectroscopic analyses of Br and I in the Sun, and abundances representative of the photosphere are derived from meteoritic abundances. However, Br and I are variable in CI chondrites, and analyses are troublesome. Anders & Grevesse (1989), following Anders & Ebihara (1982), relied on element ratios to obtain Br and I abundances. They assumed that ratios of Br/In and Br/Cd in CI chondrites are similar to those in CV and CO chondrites and type EH enstatite chondrites. Thus, using these known ratios from other chondrite groups returns the CI chondritic Br abundance if In and Cd concentrations are known in CI chondrites. For iodine, the respective ratios of I/F, I/Br, I/In, and I/Cd were used. However, these correlations do not yield Br and I abundances with smaller uncertainties than the direct determinations of Br and I in CI chondrites. Here analytical data for Br and I in CI chondrites were used to find the mean CI chondritic concentrations given in Table 3. The atomic abundances corresponding to these concentrations are chosen as representative for photospheric Br and I abundances, which, however, have more than 20% uncertainty.

#### 2.3.6. Mercury Abundance

The photospheric abundance of Hg is highly uncertain, and spectroscopic abundance determinations give  $A(\text{Hg}) < 3.0$  (Lambert, Mallia, & Warner 1969),  $A(\text{Hg}) = 0.93 \pm 0.08$  (Walter & Beer 1983), and  $A(\text{Hg}) < 1.9$  (Liumbimkov & Zalaetdinova 1987). The data spread

shows that Hg abundance determinations are unreliable for the Sun, and the Hg abundance is therefore based on meteoritic or theoretical values. However, while several Hg analyses for CI chondrites exist, the major outcome of these analyses is that they show sample contamination and the difficulty of finding clean samples in order to determine pristine Hg concentrations. Anders & Grevesse (1989) and Palme & Beer (1993) use element neutron-capture systematics to find  $N(\text{Hg}) = 0.34$  and  $0.41$ , respectively. Palme & Beer (1993) note that Orgueil samples are contaminated with Hg, but find that the theoretical Hg abundance agrees reasonably well with the Hg abundance of 310 ppb determined for the Ivuna CI chondrite. The Hg abundance in Ivuna is a single determination reported by Spettel et al. (1994). The Hg concentration listed in Table 3 is derived from three selected determinations for Ivuna of 180 ppb (Case et al. 1973), 310 ppb (Spettel et al. 1994), and 390 ppb (Reed & Jovanovic 1967), and from two determinations for Orgueil of 480 ppb (Case et al. 1973) and 210 ppb (Reed & Jovanovic 1967). The weighted average from these two meteorites ( $0.31 \pm 0.03$  ppm) is adopted as the CI chondrite group-mean Hg concentration in Table 3. This value gives  $N(\text{Hg}) = 0.413$  and  $A(\text{Hg}) = 1.16 \pm 0.04$ , which is compatible with the abundance from *r*- and *s*-process systematics. The nominal uncertainty from the statistics appears small, but the overall uncertainties in Hg analyses easily allow uncertainties of 50% ( $\pm 0.18$  dex) or more. Within these uncertainties, the meteoritic abundance is closer to the solar abundance determined by Walter & Beer (1983). Here the photospheric Hg abundance is adopted as  $A(\text{Hg}) = 1.16 \pm 0.18$  from the selected Hg analyses in CI chondrites.

### 2.4. Solar System Abundances of the Elements

The discussion in § 2 indicates that the photospheric abundances are not representative of the “bulk” Sun (or proto-Sun or solar system) because heavy-element fractionation in the Sun has altered photospheric abundances. The current and protosolar mass fractions of H, He, and the heavy elements are derived in conjunction with the photospheric He abundance in § 2.3.1.1. The results from Table 4 are used to obtain the protosolar elemental abundances (indicated by subscript “0”) from the recommended selected photospheric abundances in Table 1. The H abundances in both cases are  $A(\text{H}) = A(\text{H})_0 \equiv 12$  by definition. The He abundances on the astronomical scale are  $A(\text{He}) = 10.899$  and  $A(\text{He})_0 = 10.984$ , as given in Table 4. The protosolar abundances of all other elements are uniformly increased relative to the photospheric values using the relationship  $(Z/X)/(Z_0/X_0) = 0.8429$ . This shows that  $\sim 16\%$  heavy-element fractionation has taken place in comparison to  $\sim 18\%$  of He settling during the lifetime of the Sun. Taking the logarithm of 0.8429 relates photospheric abundances of elements heavier than He to protosolar values via

$$A(\text{El})_0 = A(\text{El}) + 0.074. \quad (5)$$

Note that the ratio  $Z/Z_0$  cannot be used to find the conversion factor because as shown in equation (1), the definition of  $A(\text{element})$  includes the element/hydrogen ratio. The resulting solar system abundances on the logarithmic scale are given in Table 2.

The protosolar abundances on the cosmochemical scale where  $N(\text{Si}) = 10^6$  atoms are derived from the abundances



on the logarithmic scale by combining equations (5) and (2),

$$\log N(\text{El})_0 = A(\text{El})_0 - 1.614. \quad (6)$$

The conversion factor for the two abundance scales of protosolar abundances is thus the sum of  $1.540 + \log 0.8429$ . Solar system abundances on the cosmochemical scale by number are also given in Table 2. On this scale, the protosolar abundances of all elements, except for H and He, are the same as photospheric abundances. This is the obvious outcome for element normalization to  $\text{Si} = 10^6$ . The protosolar H abundance is only  $\sim 0.84$  times that of the photosphere, while the respective He abundance is  $\sim 1.02$  times photospheric. The protosolar He abundance must appear slightly higher than unity on this scale because He settling from the outer layers of the Sun was slightly more efficient than that of the heavy elements, which are used for normalization of this scale. The difference in protosolar and photospheric abundances thus expresses itself either by a higher metallicity of the proto-Sun when the astronomical abundance scale is used, or by a relative depletion in hydrogen on the cosmochemical scale.

### 2.5. Abundances of the Isotopes

This section briefly describes the sources for Table 6, which lists the isotopic abundances on the cosmochemical scale for the solar system composition given in Table 2. Table 6 also lists (noted with asterisks) the abundances of radioactive and radiogenic isotopes at 4.55 Gyr ago.

Table 6 is an update from a similar table given in Anders & Grevesse (1989) and is included here because many changes in isotopic compositions of the elements have been made since then. The latest IUPAC recommended isotopic compositions of the elements are given in Rosman & Taylor (1998). These terrestrial isotopic compositions were used as representative for all elements in Table 6 except for H and the noble gases. The Sr isotopes are adjusted for an initial  $^{87}\text{Sr}/^{86}\text{Sr}$  chondritic value of 0.69885 from Minster, Birck, & Allègre (1982), and the Nd isotopes for the 4.55 Ga initial of  $^{143}\text{Nd}/^{144}\text{Nd} = 0.505906$  from data by Jacobsen & Wasserburg (1984). The Hf isotopes are modified for an initial  $^{176}\text{Hf}/^{177}\text{Hf} = 0.279628$  (Bizzarro et al. 2003). The Os isotopes reflect the  $^{187}\text{Os}/^{188}\text{Os}$  initial of 0.09530 (Chen, Papanastassiou, & Wasserburg 1998) and  $^{186}\text{Os}/^{188}\text{Os} = 0.119820$  (Walker et al. 1997) for 4.55 Ga ago. The Pb abundances correspond to the primordial Pb composition of Göpel, Manhès, & Allègre (1985).

The protosolar isotopic compositions of H and the noble gases were recently reviewed by Wieler (2002), and his results are adopted here. The hydrogen isotopic composition is taken from the D/H ratio of  $1.94(\pm 0.39) \times 10^{-5}$ , and for helium, the  $^3\text{He}/^4\text{He}$  ratio of  $1.66(\pm 0.05) \times 10^{-4}$  as determined for Jupiter's atmosphere is taken as a representative protosolar value. The Ne, Ar, Kr, and Xe isotopic compositions are taken from the isotope ratios given for the solar wind by Wieler (2002).

## 3. CONDENSATION TEMPERATURES OF THE ELEMENTS

Having established the abundances of the elements in the previous sections, their condensation temperatures are calculated next. There are two abundance sets of the elements (photospheric and protosolar), and condensation tempera-

tures will be different for each set, as they have different slightly metallicity. Therefore, the question is, which abundance set should be used to calculate condensation temperatures? The solar system (or protosolar) abundances should be used for modeling chemistry in the solar nebula and other systems of solar metallicity. Condensation temperatures for the photospheric abundance set are not directly applicable to the solar nebula because of the slightly lower metallicity caused by gravitational settling of the elements from the photosphere. However, the photospheric elemental abundances are used as a standard reference for abundance normalization in other stars, so one may want a self-consistent set of abundances and condensation temperatures for comparisons. Therefore, condensation temperatures were computed for both abundance sets.

The condensation temperatures and the 50% condensation temperatures are calculated for all elements at a total pressure of  $10^{-4}$  bar. This pressure was chosen because it is characteristic for the total pressure near 1 AU in the solar nebula (see Fegley 2000). Many of the previously computed condensation temperatures of the elements are also computed for this total pressure, which facilitates comparison of the computations (see, e.g., Larimer 1967, 1973; Grossman 1972; Grossman, & Larimer 1974; Boynton 1975; Wai & Wasson 1977, 1979; Sears 1978; Fegley & Lewis 1980; Saxena & Eriksson 1983; Fegley & Palme 1985; Kornacki & Fegley 1986; Palme & Fegley 1990; Ebel & Grossman 2000). The next sections give technical notes on condensation calculations, the condensates of the major elements (hereafter also called rock-forming elements), condensation chemistry of the minor and trace elements, and the condensation chemistry of ices.

### 3.1. Computational Methods and Nomenclature

The chemical equilibrium condensation temperatures are computed with the CONDOR code (e.g., Lodders & Fegley 1993, 1995, 1997; Fegley & Lodders 1994). The advantage of using the CONDOR code is that the chemistry of *all* elements is considered simultaneously. This is important because the chemistry (species in the gas, type of condensate) of minor elements is affected by that of major elements.

The condensation temperature of Al, Fe, or any other another element is determined by the total pressure, the elemental abundances that determine the partial pressures in the gas, the distribution of an element between different gases and condensates, and the vapor pressure of the element. The CONDOR computer program considers these factors in the calculations. The code operates by simultaneously solving for mass balance and chemical equilibrium for 2000 gases and 1600 condensates of all naturally occurring elements.

In the case of Al, the total abundance of Al in all forms is  $n(\text{Al})$ , which is the protosolar or photospheric abundance of Al. The total mole fraction ( $X$ ) of Al is then

$$X_{\Sigma\text{Al}} = \frac{n(\text{Al})}{n(\text{H} + \text{H}_2 + \text{He})}, \quad (7)$$

where  $n(\text{H} + \text{H}_2 + \text{He})$  is the sum of the H and He abundances with the temperature-dependent H and  $\text{H}_2$  equilibrium taken into account. In the actual computation, other gases such as CO,  $\text{H}_2\text{O}$ ,  $\text{N}_2$ , Ne, ions, etc., are also included in the

denominator, but these are neglected in the description here for clarity.

Multiplying  $X_{\Sigma\text{Al}}$  by the total pressure  $P_{\text{tot}}$  gives the pressure of Al in all forms, which is equal to the partial pressure sum for Al,

$$P_{\Sigma\text{Al}} = X_{\Sigma\text{Al}}P_{\text{tot}} = P_{\text{Al}} + P_{\text{AlO}} + P_{\text{AlOH}} + \dots \quad (8)$$

Equation (8) can be rewritten in terms of the thermodynamic activity of Al ( $a_{\text{Al}}$ ), the equilibrium constants ( $K_i$ ) for forming the Al gases from the constituent elements in their reference states, and the thermodynamic activities and fugacities of other elements combined with Al in gases,

$$P_{\Sigma\text{Al}} = X_{\Sigma\text{Al}}P_{\text{tot}} = a_{\text{Al}}[K_{\text{Al}} + K_{\text{AlO}}f_{\text{O}_2}^{0.5} + K_{\text{AlOH}}(f_{\text{O}_2}f_{\text{H}_2})^{0.5} + \dots] \quad (9)$$

The actual mass balance sum for Al in the CONDOR code includes  $\sim 80$  Al-bearing gases. The most important ones in a solar composition gas are Al and AlOH, followed by  $\text{Al}_2\text{O}$ , AlH, AlF, and AlCl. Analogous forms of equation (9) are written for each element in the code. The equilibrium constants ( $K_i$ ) in the equations are taken from thermodynamic data compilations such as the JANAF tables (Chase 1999), Gurvich, Veys, & Alcock (1989), and the primary thermodynamic literature. The majority of the thermodynamic data sources used are listed in Fegley & Lodders (1994) and Lodders & Fegley (1993). Some updates to our thermodynamic database have been published (Lodders 1999, 2003), and others are in publication in the near future.

Equation (9) shows that the chemistry of the elements is coupled, and the mass balance equations from the set of coupled, nonlinear equations are solved iteratively. An initial guess is assumed for the activity or fugacity of each element. These guesses can be optimized if the major gas for each element is known, but this is not necessary for the code to operate properly. CONDOR solves the set of mass balance equations and returns the thermodynamic activity or fugacity for each element, the abundances of all gases (molecules, radicals, atoms, ions) included in the code, and information on the quality of the calculated results for each element. The convergence criterion requires that the calculated and input abundances for each element agree to within 1 part in  $10^{15}$ .

Condensate stabilities are computed considering compound formation from the elements in their respective reference states. For example, the reaction



is used for corundum. Condensation occurs when the thermodynamic activity of  $\text{Al}_2\text{O}_3$  reaches unity, and this is calculated from

$$a_{\text{Al}_2\text{O}_3} = a_{\text{Al}}^2 f_{\text{O}_2}^{1.5} K_{\text{Al}_2\text{O}_3}, \quad (11)$$

where  $K_{\text{Al}_2\text{O}_3}$  is the temperature-dependent equilibrium constant for corundum, and  $a_{\text{Al}}$  and  $f_{\text{O}_2}$  are taken from the gas-phase equilibrium calculations described above. The activities of all other possible condensates are computed in a similar fashion. (The concept of activity is defined in many thermodynamic textbooks, such as Lewis & Randall 1961.) At the temperature at which the thermodynamic activity of a pure phase (e.g., Fe-metal, corundum [ $\text{Al}_2\text{O}_3$ ], iron sulfide

[FeS]) reaches unity, the compound or element begins to condense from the gas phase. In the following discussion, this temperature is referred to as ‘‘appearance condensation temperature,’’ or just ‘‘condensation temperature,’’ which is different from the 50% condensation temperature described below.

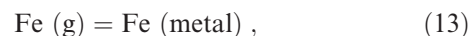
Once corundum is stable, the fraction of Al ( $\alpha_{\text{Al}}$ ) condensed in corundum is calculated and the gas-phase abundance of Al ( $P_{\Sigma\text{Al}}$ ) is reduced by multiplying by  $(1 - \alpha_{\text{Al}})$  (see also Palme & Fegley 1990 for this procedure). Analogous corrections are made for all elements distributed between the gas and condensates. The gas-phase and gas-solid chemical equilibria are coupled and solved simultaneously using iterative techniques.

Equations (9) and (11) show that the Al chemistry is affected by the oxygen fugacity, which depends on the distribution of oxygen between CO,  $\text{H}_2\text{O}$ , SiO, and other O-bearing gases. The mass-balance sum for oxygen is

$$P_{\Sigma\text{O}} = X_{\Sigma\text{O}}P_{\text{tot}} = 2f_{\text{O}_2} + f_{\text{O}_2}^{0.5}[K_{\text{CO}}a_{\text{C}} + K_{\text{H}_2\text{O}}f_{\text{H}_2} + K_{\text{SiO}}a_{\text{Si}} + \dots], \quad (12)$$

where  $a_{\text{C}}$  and  $a_{\text{Si}}$  are the thermodynamic activities of carbon and silicon. Because the solar O/C and O/Si atomic ratios are  $\sim 2$  and  $\sim 14$ , respectively, SiO is less important than CO and  $\text{H}_2\text{O}$  for controlling the  $f_{\text{O}_2}$  to a good first approximation. The  $\text{H}_2\text{O}/\text{H}_2$  ratio is a convenient proxy for the oxygen fugacity. The  $\text{H}_2\text{O}/\text{H}_2$  ratio of the solar system composition gas is about  $5.0 \times 10^{-4}$ , roughly half of  $9.2 \times 10^{-4}$  resulting from the solar abundances given by Anders & Grevesse (1989). This means that at constant temperature, the thermodynamic activity of corundum from equation (11) is lower for the solar system composition here than for that given in Anders & Grevesse (1989). In turn, the condensation temperature of corundum are also lower because  $a_{\text{Al}_2\text{O}_3}$  reaches unity only at lower temperatures when the temperature-dependent equilibrium constant becomes larger.

The condensation temperatures of other elements (e.g., Ca, Mg, Ti, Si) which condense as oxides and silicates are affected in a similar manner by the new oxygen fugacity. However, for some elements like Fe and Ni, the gas chemistry is essentially independent of  $f_{\text{O}_2}$ . For example, monatomic Fe is the dominant Fe gas ( $P_{\Sigma\text{Fe}} \approx P_{\text{Fe}}$ ), and the condensation reaction is



for which the equilibrium constant is

$$\log(K_{\text{Fe}}) = \log(a_{\text{Fe}}/P_{\text{Fe}}) = A + B/T, \quad (14)$$

where  $A$  and  $B$  are fit coefficients that describe the temperature dependence of the equilibrium constant in a simplified form. The iron condensation temperature follows from the requirement of  $a_{\text{Fe}} \equiv 1 = K_{\text{Fe}}P_{\text{Fe}}$ , so that

$$-\log P_{\text{Fe}} = A + B/T. \quad (15)$$

The reverse of reaction (13) is the vaporization reaction of Fe metal to Fe (g), for which the vapor pressure equation is  $\log P_{\text{vap}} = A' + B'/T$ , with  $A' = -A$  and  $B' = -B$ . Hence, the equilibrium condensation temperature is the temperature at which the gas partial pressure ( $P_i$ ) equals the vapor pressure ( $P_{\text{vap}}$ ) of the condensing species. In other words, the saturation ratio  $S = P_i/P_{\text{vap}} = 1$  equals the thermodynamic activity  $a_i$ .



For calculating standard condensation temperatures, condensates remain in equilibrium with the gas as temperature drops. This means that the first (primary) condensates can react with the gas to form secondary condensates at lower temperatures. This scenario applies to physical settings such as the solar nebula, protostellar and protoplanetary disks, and stellar outflows such as those around mass-losing giant stars. However, this condensation sequence does not apply to giant planetary, brown dwarf, or cool stellar atmospheres, in which gravitational settling removes primary condensates into cloud layers from cooler gas, preventing the formation of secondary condensates.

The condensation temperatures of minor and trace elements that do not condense as pure phases are computed differently. Many minor and trace elements condense by forming (solid) solutions with host phases made of major elements. For example, iron metal is the host phase for other less abundant metals such as Ni, Co, Ge, or Au. The formation of solid solutions starts when a host phase begins to condense and the minor and trace elements condensing into a host phase have the same condensation temperatures as the host phase itself. On the other hand, the “50% condensation temperature” is a better indication of the extent of condensation or volatility of minor and trace elements and can be computed for major elements as well. At this temperature, half of an element is in the gas and the other half is sequestered into condensates. For example, Ni and Ge both start to condense into Fe metal as soon as Fe metal forms, but 50% of all Ni is condensed in Fe alloy at higher temperatures than 50% of all Ge, which is more volatile. However, it should be noted that the 50% condensation temperatures of trace elements are independent of their total solar system abundance but are dependent on the availability and amount of the major host phase, which do depend on the relative abundances of the major elements.

The selection of host phases for trace element solutions is guided by elemental analyses of minerals in meteorites (see § 3.3). Other indicators of which mineral phases can serve as host phases are general chemical affinities of the elements and phase equilibrium studies done in materials science. The calculation of the 50% condensation temperatures of trace elements also involves the application of activity coefficients in order to take non-ideal solid solutions in a host phase into account. The importance of activity coefficients and their application to condensation temperatures was explored in detail by Larimer (e.g., see Larimer 1967, 1973, 1988) and many in subsequent studies (e.g., Wai & Wasson 1977, 1979; Wasson 1985; Sears 1978; Fegley & Lewis 1980; Kornacki & Fegley 1986 and references therein). Details of the procedure of solid-solution computations applied here are described by Kornacki & Fegley (1986). When available, activity coefficients were taken from and applied as in the previous condensation studies listed above.

### 3.2. Major Element Condensates

Condensation of the major elements (Al, Ca, Mg, Si, Fe) and other important rock-forming elements (Ti, S, P) is described first because they form the bulk of rocky material, and their condensates serve as host phases for minor and trace elements. The elements H, C, N, O, and the noble gases belong to the major elements, but they condense only at very low temperatures (with the exception of ~23% of all oxygen condensing into rock) and are treated separately

TABLE 7  
MAJOR ELEMENT CONDENSATION TEMPERATURES

Ideal Formula	Mineral Name	Solar System Composition (K)	Photospheric Composition (K)
Al <sub>2</sub> O <sub>3</sub> .....	Corundum	1677	1665
CaAl <sub>12</sub> O <sub>19</sub> .....	Hibonite	1659	1647
CaAl <sub>4</sub> O <sub>7</sub> .....	Grossite	1542	1531
Ca <sub>2</sub> Al <sub>2</sub> SiO <sub>7</sub> .....	Gehlenite	1529	1519
CaTiO <sub>3</sub> .....	Perovskite	1593	1584
Ca <sub>4</sub> Ti <sub>3</sub> O <sub>10</sub> .....	Ca titanate	1578	1567
Ca <sub>3</sub> Ti <sub>2</sub> O <sub>7</sub> .....	Ca titanate	1539	1529
Ca <sub>4</sub> Ti <sub>3</sub> O <sub>10</sub> .....	Ca titanate	1512	1502
CaTiO <sub>3</sub> .....	Perovskite	1441	1429
MgAl <sub>2</sub> O <sub>4</sub> .....	Spinel	1397	1387
CaAl <sub>2</sub> Si <sub>2</sub> O <sub>8</sub> .....	Anorthite	1387	1378
Mg <sub>2</sub> SiO <sub>4</sub> .....	Forsterite	1354	1346
MgSiO <sub>3</sub> .....	Enstatite	1316	1308
CaMgSi <sub>2</sub> O <sub>6</sub> .....	Diopside	1347	1339
Fe .....	Fe alloy	1357	1351
Fe <sub>3</sub> P .....	Schreibersite	1248	1245
FeS .....	Troilite	704	693
Fe <sub>3</sub> O <sub>4</sub> .....	Magnetite	371	365
H <sub>2</sub> O .....	Water ice	182	181

NOTE.—At 10<sup>-4</sup> bar total pressure.

(§ 3.4). Table 7 summarizes the condensation sequence of some major elements for the solar system and photospheric compositions. The condensation temperatures for the solar system composition with higher metallicity are generally somewhat larger (about 10 K) than those calculated for the photospheric composition. Because condensation sequences are similar for both compositions, the following discussion uses condensation temperatures for the solar system abundances.

The most refractory major condensates are Ca-Al-Ti-bearing compounds. These phases are well known to occur in chondrites as Ca-Al-rich inclusions (CAIs), which likely represent the first condensates in the solar nebula. With dropping temperatures, the initial Ca-Al-rich phases (corundum, hibonite, grossite) are converted to gehlenite, the Al-rich end member of the gehlenite-akermanite solid solution (Ca<sub>2</sub>Al<sub>2</sub>SiO<sub>7</sub>-Ca<sub>2</sub>MgSi<sub>2</sub>O<sub>7</sub>) called melilite. This is followed by the appearance of anorthite (the Ca-rich member of feldspar) and spinel, which remove more Al, Ca, Si, and Mg from the gas. The first Si-bearing condensate is gehlenite, and the first Mg-bearing condensates are melilite and spinel. However, very little Si and Mg is incorporated into melilite and spinel, and major removal of Mg and Si from the gas begins with the condensation of forsterite (Mg<sub>2</sub>SiO<sub>4</sub>) and enstatite (MgSiO<sub>3</sub>).

The condensation temperature of metallic iron is close to that of forsterite. Condensation of the three most abundant rock-forming elements, Mg, Si, and Fe, occurs together over a relatively small (~100 K) temperature interval (Table 7). Si, Mg, and Fe are often called “common elements” (Larimer 1988) because these elements and their condensation temperature range are used as reference to define “refractory elements” (elements condensing at higher *T* than Mg, Si, and Fe) and “volatile elements” (condensing at lower *T* than Mg, Si, and Fe).

The last major rocky condensate that removes sulfur from the gas is troilite. It forms from the condensed Fe alloy and H<sub>2</sub>S gas ~650 K below the condensation temperature

of the Fe alloy. Troilite condensation serves as a benchmark to further divide volatile elements: elements condensing between common elements and troilite are called “moderately volatile,” and elements condensing below troilite are “volatile” or “highly volatile.” Here the term “highly volatile” is reserved for H, C, N, O, and noble gases, for which the condensation temperatures of magnetite at 371 K and water at 182 K (see § 3.4) serve as temperature marks. The volatility classifications of the more abundant rock-forming elements are: refractory (Ca, Al, Ti), common (Fe, Si, Mg), moderately volatile (P), volatile (S), and highly volatile (H, C, N, O, noble gases).

### 3.3. Minor and Trace Element Condensation

Tables 8 and 9 give condensation temperatures for all elements and the names of the phase(s) or host(s) for 50% trace element condensation. Appearance condensation temperatures are only listed for the major elements and very refractory elements in Tables 8 and 9. The latter are given because their compounds can condense prior to any major condensate host. The initial phase formed is given for these “pure” compounds. For elements condensing into solid solution with a major element host phase, the dissolving compound assumed in the computations is listed in braces.

TABLE 8  
EQUILIBRIUM CONDENSATION TEMPERATURES FOR A SOLAR-SYSTEM COMPOSITION GAS

Element (1)	$T_C$ (K) (2)	Initial Phase {Dissolving Species} (3)	50% $T_C$ (K) (4)	Major Phase(s) or Host(s) (5)
H	182	H <sub>2</sub> O ice	...	...
He	<3	He ice	...	...
Li		{Li <sub>4</sub> SiO <sub>4</sub> , Li <sub>2</sub> SiO <sub>3</sub> }	1142	Forsterite + enstatite
Be		{BeCa <sub>2</sub> Si <sub>2</sub> O <sub>7</sub> }	1452	Melilite
B		{CaB <sub>2</sub> Si <sub>2</sub> O <sub>8</sub> }	908	Feldspar
C	78	CH <sub>4</sub> ·7H <sub>2</sub> O	40	CH <sub>4</sub> ·7H <sub>2</sub> O + CH <sub>4</sub> ice
N	131	NH <sub>3</sub> ·H <sub>2</sub> O	123	NH <sub>3</sub> ·H <sub>2</sub> O
O	182	Water ice <sup>a</sup>	180	rock + water ice
F	739	Ca <sub>5</sub> [PO <sub>4</sub> ] <sub>3</sub> F	734	F apatite
Ne	9.3	Ne ice	9.1	Ne ice
Na		{NaAlSi <sub>3</sub> O <sub>8</sub> }	958	Feldspar
Mg	1397	Spinel		
	1354	Forsterite <sup>b</sup>	1336	Forsterite
Al	1677	Al <sub>2</sub> O <sub>3</sub>	1653	Hibonite
Si	1529	Gehlenite		
	1354	Forsterite <sup>b</sup>	1310	Forsterite + enstatite
P	1248	Fe <sub>3</sub> P	1229	Schreibersite
S	704	FeS	664	Troilite
Cl	954	Na <sub>4</sub> [Al <sub>3</sub> Si <sub>3</sub> O <sub>12</sub> ]Cl	948	Sodalite
Ar	48	Ar·6H <sub>2</sub> O	47	Ar·6H <sub>2</sub> O
K		{KAlSi <sub>3</sub> O <sub>8</sub> }	1006	Feldspar
Ca	1659	CaAl <sub>12</sub> O <sub>19</sub>	1517	Hibonite + gehlenite
Sc		{Sc <sub>2</sub> O <sub>3</sub> }	1659	Hibonite
Ti	1593	CaTiO <sub>3</sub>	1582	Titanate
V		{VO, V <sub>2</sub> O <sub>3</sub> }	1429	Titanate
Cr		{Cr}	1296	Fe alloy
Mn		{Mn <sub>2</sub> SiO <sub>4</sub> , MnSiO <sub>3</sub> }	1158	Forsterite + enstatite
Fe	1357 <sup>c</sup>	Fe metal <sup>c</sup>	1334	Fe alloy
Co		{Co}	1352	Fe alloy
Ni		{Ni}	1353	Fe alloy
Cu		{Cu}	1037	Fe alloy
Zn		{Zn <sub>2</sub> SiO <sub>4</sub> , ZnSiO <sub>3</sub> }	726	Forsterite + enstatite
Ga		{Ga, Ga <sub>2</sub> O <sub>3</sub> }	968	Fe alloy + feldspar
Ge		{Ge}	883	Fe alloy
As		{As}	1065	Fe alloy
Se		{FeSe <sub>0.96</sub> } <sup>d</sup>	697	Troilite
Br		{CaBr <sub>2</sub> }	546	Cl apatite
Kr	53	Kr·6H <sub>2</sub> O	52	Kr·6H <sub>2</sub> O
Rb		{Rb silicate}	800	Feldspar
Sr		{SrTiO <sub>3</sub> }	1464	Titanate
Y		{Y <sub>2</sub> O <sub>3</sub> }	1659	Hibonite
Zr	1764	ZrO <sub>2</sub>	1741	ZrO <sub>2</sub>
Nb		{NbO, NbO <sub>2</sub> }	1559	Titanate
Mo		{Mo}	1590	Refractory metal alloy
Ru		{Ru}	1551	Refractory metal alloy
Rh		{Rh}	1392	Refractory metal alloy
Pd		{Pd}	1324	Fe alloy

TABLE 8—Continued

Element (1)	$T_C$ (K) (2)	Initial Phase {Dissolving Species} (3)	50% $T_C$ (K) (4)	Major Phase(s) or Host(s) (5)
Ag.....		{Ag}	996	Fe alloy
Cd.....		{CdSiO <sub>3</sub> , CdS}	652	Enstatite + troilite
In.....		{InS, InSe, InTe}	536	FeS
Sn.....		{Sn}	704	Fe alloy
Sb.....		{Sb}	979	Fe alloy
Te.....		{Te}	709	Fe alloy
I.....		{CaI <sub>2</sub> }	535	Cl apatite
Xe.....	69	Xe·6H <sub>2</sub> O	68	Xe·6H <sub>2</sub> O
Cs.....		{Cs silicate}	799	Feldspar
Ba.....		{BaTiO <sub>3</sub> }	1455	Titanate
La.....		{La <sub>2</sub> O <sub>3</sub> }	1578	Hibonite + titanate
Ce.....		{CeO <sub>2</sub> , Ce <sub>2</sub> O <sub>3</sub> }	1478	Hibonite + titanate
Pr.....		{Pr <sub>2</sub> O <sub>3</sub> }	1582	Hibonite + titanate
Nd.....		{Nd <sub>2</sub> O <sub>3</sub> }	1602	Hibonite
Sm.....		{Sm <sub>2</sub> O <sub>3</sub> }	1590	Hibonite + titanate
Eu.....		{EuO, Eu <sub>2</sub> O <sub>3</sub> }	1356	Hibonite + titanate + feldspar
Gd.....		{Gd <sub>2</sub> O <sub>3</sub> }	1659	Hibonite
Tb.....		{Tb <sub>2</sub> O <sub>3</sub> }	1659	Hibonite
Dy.....		{Dy <sub>2</sub> O <sub>3</sub> }	1659	Hibonite
Ho.....		{Ho <sub>2</sub> O <sub>3</sub> }	1659	Hibonite
Er.....		{Er <sub>2</sub> O <sub>3</sub> }	1659	Hibonite
Tm.....		{Tm <sub>2</sub> O <sub>3</sub> }	1659	Hibonite
Yb.....		{Yb <sub>2</sub> O <sub>3</sub> }	1487	Hibonite + titanate
Lu.....		{Lu <sub>2</sub> O <sub>3</sub> }	1659	hibonite
Hf.....	1703	HfO <sub>2</sub>	1684	HfO <sub>2</sub>
Ta.....		{Ta <sub>2</sub> O <sub>5</sub> }	1573	Hibonite + titanate
W.....		{W}	1789	Refractory metal alloy
Re.....		{Re}	1821	Refractory metal alloy
Os.....		{Os}	1812	Refractory metal alloy
Ir.....		{Ir}	1603	Refractory metal alloy
Pt.....		{Pt}	1408	Refractory metal alloy
Au.....		{Au}	1060	Fe alloy
Hg.....		{HgS, HgSe, HgTe}	252	Troilite
Tl.....		{Tl <sub>2</sub> S, Tl <sub>2</sub> Se, Tl <sub>2</sub> Te}	532	Troilite
Pb.....		{Pb}	727	Fe alloy
Bi.....		{Bi}	746	Fe alloy
Th.....		{ThO <sub>2</sub> }	1659	Hibonite
U.....		{UO <sub>2</sub> }	1610	Hibonite

NOTE.—At  $10^{-4}$  bar total pressure. Solar system abundances from Table 2.

<sup>a</sup> 22.75% of oxygen is condensed into rock before water ice condensation.

<sup>b</sup> Major condensed reservoir of element.

<sup>c</sup> Condensation temperature of pure iron metal.

<sup>d</sup> Modeling assumes solution of FeSe<sub>0.96</sub> for which reliable thermodynamic properties exist, instead of FeSe.

The condensation chemistry of minor and trace elements is governed by their geochemical affinities and by the presence of a suitable condensed host phase. Trace element analyses in meteoritic minerals are used as a guide to which major minerals may serve as host phases during condensation (e.g., Allen & Mason 1973; Mason & Graham 1970). However, the host minerals in meteorites may only preserve the “final” product of the condensation sequence, leaving aside any subsequent changes from mineral processing and alteration on the meteorite parent body after accretion of nebular condensates. For example, a trace element may condense into Fe metal but later transfer from metal into troilite once troilite begins to form because the element has more chalcophile (sulfide-loving) than siderophile (metal-loving) tendencies. Such possible redistribution will be mentioned in the following sections, which describe minor and trace element condensation into the major element host phases.

### 3.3.1. Ultrarefractory Trace Element Condensation: W, Re, Os, Ir, Mo, Pt, Rh, Ru, Zr, and Hf

Several transition elements condense before any major condensate (§ 3.2) forms. The transition metals W, Re, Os, Ir, Mo, Pt, Rh, and Ru condense before iron metal. Refractory metal nuggets and objects known as “fremdlinge” (little strangers) in refractory inclusions in meteorites are composed of these elements. Tables 8 and 9 list the 50% condensation temperatures for condensation into a refractory alloy, computed in a similar manner as done before by Fegley & Palme (1985). The refractory metal 50% condensation temperatures are essentially the same as those obtained by Fegley & Palme (1985), which is not too surprising because the H<sub>2</sub>O/H<sub>2</sub> ratio of  $5 \times 10^{-4}$  applied in their calculations is identical to that obtained here for a solar system composition gas.

TABLE 9  
EQUILIBRIUM CONDENSATION TEMPERATURES FOR A SOLAR-PHOTOSPHERE COMPOSITION GAS

Element (1)	$T_C$ (K) (2)	Initial Phase {Dissolving Species} (3)	$50\% T_C$ (K) (4)	Major Phase(s) or Host(s) (5)
H .....	181	H <sub>2</sub> O ice	...	...
He .....	< 3	He ice	...	...
Li .....		{Li <sub>4</sub> SiO <sub>4</sub> , Li <sub>2</sub> SiO <sub>3</sub> }	1135	Forsterite + enstatite
Be .....		{BeCa <sub>2</sub> Si <sub>2</sub> O <sub>7</sub> }	1445	Melilite
B .....		{CaB <sub>2</sub> Si <sub>2</sub> O <sub>8</sub> }	906	Feldspar
C .....	77	CH <sub>4</sub> ·7H <sub>2</sub> O	40	CH <sub>4</sub> ·7H <sub>2</sub> O + CH <sub>4</sub> ice
N .....	131	NH <sub>3</sub> ·H <sub>2</sub> O	123	NH <sub>3</sub> ·H <sub>2</sub> O
O .....	181	water ice <sup>a</sup>	179	Rock + water ice
F .....	731	Ca <sub>5</sub> [PO <sub>4</sub> ] <sub>3</sub> F	726	F apatite
Ne .....	9.3	Ne ice	9.1	Ne ice
Na .....		{NaAlSi <sub>3</sub> O <sub>8</sub> }	953	Feldspar
Mg .....	1387	spinel		
	1346	forsterite <sup>b</sup>	1327	Forsterite
Al .....	1665	Al <sub>2</sub> O <sub>3</sub>	1641	Hibonite
Si .....	1519	gehlenite		
	1346	forsterite <sup>b</sup>	1302	Forsterite + enstatite
P .....	1245	Fe <sub>3</sub> P	1226	Schreibersite
S .....	693	FeS	655	Troilite
Cl .....	948	Na <sub>4</sub> [Al <sub>3</sub> Si <sub>3</sub> O <sub>12</sub> ]Cl	940	Sodalite
Ar .....	48	Ar·6H <sub>2</sub> O	47	Ar·6H <sub>2</sub> O
K .....		{KAlSi <sub>3</sub> O <sub>8</sub> }	1001	feldspar
Ca .....	1647	hibonite	1505	Hibonite + gehlenite
Sc .....		{Sc <sub>2</sub> O <sub>3</sub> }	1647	Hibonite
Ti .....	1584	CaTiO <sub>3</sub>	1573	Titanate
V .....		{VO, V <sub>2</sub> O <sub>3</sub> }	1427	Hibonite + titanate
Cr .....		{Cr}	1291	Fe alloy
Mn .....		{Mn <sub>2</sub> SiO <sub>4</sub> , MnSiO <sub>3</sub> }	1150	Forsterite + enstatite
Fe .....	1351 <sup>c</sup>	Fe metal <sup>c</sup>	1328	Fe alloy
Co .....		{Co}	1347	Fe alloy
Ni .....		{Ni}	1348	Fe alloy
Cu .....		{Cu}	1033	Fe alloy
Zn .....		{Zn <sub>2</sub> SiO <sub>4</sub> , ZnSiO <sub>3</sub> }	723	Forsterite + enstatite
Ga .....		{Ga, Ga <sub>2</sub> O <sub>3</sub> }	971	Fe alloy + feldspar
Ge .....		{Ge}	885	Fe alloy
As .....		{As}	1061	Fe alloy
Se .....		{FeSe <sub>0.96</sub> } <sup>d</sup>	688	Troilite
Br .....		{CaBr <sub>2</sub> }	544	F apatite
Kr .....	53	Kr·6H <sub>2</sub> O	52	Kr·6H <sub>2</sub> O
Rb .....		{Rb silicate}	798	Feldspar
Sr .....		{SrTiO <sub>3</sub> }	1455	Hibonite + titanate
Y .....		{Y <sub>2</sub> O <sub>3</sub> }	1647	Hibonite
Zr .....	1758	ZrO <sub>2</sub>	1736	ZrO <sub>2</sub>
Nb .....		{NbO, NbO <sub>2</sub> }	1557	Titanate
Mo .....		{Mo}	1587	Refractory metal alloy
Ru .....		{Ru}	1546	Refractory metal alloy
Rh .....		{Rh}	1387	Refractory metal alloy
Pd .....		{Pd}	1318	Fe alloy
Ag .....		{Ag}	992	Fe alloy
Cd .....		{CdSiO <sub>3</sub> , CdS}	650	Enstatite + troilite
In .....		{InS, InSe, InTe}	535	Troilite
Sn .....		{Sn}	703	Fe alloy
Sb .....		{Sb}	976	Fe alloy
Te .....		{Te}	705	Fe alloy
I .....		{CaI <sub>2</sub> }	533	F apatite
Xe .....	69	Xe·6H <sub>2</sub> O	68	Xe·6H <sub>2</sub> O
Cs .....		{Cs silicate}	797	Feldspar
Ba .....		{BaTiO <sub>3</sub> }	1447	Titanate
La .....		{La <sub>2</sub> O <sub>3</sub> }	1570	Hibonite + titanate
Ce .....		{CeO <sub>2</sub> , Ce <sub>2</sub> O <sub>3</sub> }	1477	Hibonite + titanate
Pr .....		{Pr <sub>2</sub> O <sub>3</sub> }	1574	Hibonite + titanate
Nd .....		{Nd <sub>2</sub> O <sub>3</sub> }	1594	Hibonite
Sm .....		{Sm <sub>2</sub> O <sub>3</sub> }	1580	Hibonite + titanate
Eu .....		{EuO, Eu <sub>2</sub> O <sub>3</sub> }	1347	Hibonite + titanate + feldspar

TABLE 9—Continued

Element (1)	$T_C$ (K) (2)	Initial Phase {Dissolving Species} (3)	50% $T_C$ (K) (4)	Major Phase(s) or Host(s) (5)
Gd		{Gd <sub>2</sub> O <sub>3</sub> }	1647	Hibonite
Tb		{Tb <sub>2</sub> O <sub>3</sub> }	1647	Hibonite
Dy		{Dy <sub>2</sub> O <sub>3</sub> }	1647	Hibonite
Ho		{Ho <sub>2</sub> O <sub>3</sub> }	1647	Hibonite
Er		{Er <sub>2</sub> O <sub>3</sub> }	1647	Hibonite
Tm		{Tm <sub>2</sub> O <sub>3</sub> }	1647	Hibonite
Yb		{Yb <sub>2</sub> O <sub>3</sub> }	1475	Hibonite + titanate
Lu		{Lu <sub>2</sub> O <sub>3</sub> }	1647	Hibonite
Hf	1694	HfO <sub>2</sub>	1676	HfO <sub>2</sub>
Ta		{Ta <sub>2</sub> O <sub>5</sub> }	1565	Hibonite + titanate
W		{W}	1790	Refractory metal alloy
Re		{Re}	1817	Refractory metal alloy
Os		{Os}	1808	Refractory metal alloy
Ir		{Ir}	1598	Refractory metal alloy
Pt		{Pt}	1403	Refractory metal alloy
Au		{Au}	1061	Fe alloy
Hg		{HgS, HgSe, HgTe}	250	Troilite
Tl		{Tl <sub>2</sub> S, Tl <sub>2</sub> Se, Tl <sub>2</sub> Te}	531	Troilite
Pb		{Pb}	724	Fe alloy
Bi		{Bi}	743	Fe alloy
Th		{ThO <sub>2</sub> }	1647	Hibonite
U		{UO <sub>2</sub> }	1604	Hibonite

NOTE.—At 10<sup>-4</sup> bar total pressure. Photospheric abundances from Table 1.

<sup>a</sup> 22.75% of oxygen is condensed into rock before water ice condensation.

<sup>b</sup> Major condensed reservoir of element.

<sup>c</sup> Condensation temperature of pure iron metal.

<sup>d</sup> Modeling assumes solution of FeSe<sub>0.96</sub> for which reliable thermodynamic properties exist, instead of FeSe.

Refractory lithophile (rock-loving) elements that condense as oxides before any major element oxide host include Zr, Hf, Y, and Sc (e.g., Kornacki & Fegley 1986). At the total pressure chosen here, only HfO<sub>2</sub> and ZrO<sub>2</sub> condense before the first potential host, hibonite, appears. The possible solid solution of HfO<sub>2</sub> into ZrO<sub>2</sub> is not considered here. The condensation temperature of pure Sc<sub>2</sub>O<sub>3</sub> is a few degrees below that of hibonite, and Sc enters this host instead of forming “pure” Sc<sub>2</sub>O<sub>3</sub>. However, at higher total pressure, Sc and Y would behave like Hf and Zr.

### 3.3.2. Lithophile Elements Condensing into Ca Titanates and Hibonite: Ba, Sr, Sc, Y, V, Nb, Ta, Th, U, and Rare Earth Elements

The calcium titanates (perovskite [CaTiO<sub>3</sub>], Ca<sub>4</sub>Ti<sub>3</sub>O<sub>10</sub>, Ca<sub>3</sub>Ti<sub>2</sub>O<sub>7</sub>) and the Ca aluminate hibonite (CaAl<sub>12</sub>O<sub>19</sub>) are initial host phases for condensation of rare earth elements (REE) and lithophile elements such as Ba, Sr, Sc, Y, V, Nb, Ta, Th, and U (e.g., Boynton 1975; Kornacki & Fegley 1986). Hibonite condenses first, and several of the more refractory trace elements (e.g., Sc, Y, Th, U, heavy REE) are 50% condensed into hibonite before perovskite appears. The somewhat less refractory elements (V, Nb, Ta, light REE, Sr, Ba) condense to 50% once perovskite (or another Ca titanate) is present as an additional host. The most volatile element in this group is Eu, which is condensed by 50% when feldspar is stable.

### 3.3.3. Lithophile Element Condensation in Melilite: Be

Melilite, the solid solution of gehlenite and akermanite, serves as host phase for initial Be condensation (Lauretta & Lodders 1997), into which 50% of Be is condensed at 1421 K.

### 3.3.4. Lithophile Elements Condensing into Olivine (Forsterite) and Pyroxene (Enstatite): Cd, Li, Mn, and Zn

Meteorite analyses show that Li, Mn, Zn, and Cd are compatible with Mg silicates. Here forsterite, the Mg end member of the olivine group, and enstatite, the Mg-rich end member of the pyroxene group, serve as condensation hosts for these elements. Forsterite condensation initiates condensation of Li, Mn, Zn, and Cd, which continue to condense into enstatite once the conversion of forsterite to enstatite begins at lower temperature. The trace elements Mn, Li, and Zn are more volatile than Mg and Si, and their 50% condensation temperatures are much lower (by 150–570 K) than those of Mg and Si (Tables 8 and 9). Cadmium, which chemically follows Zn, is the most volatile element in this group and is more chalcophile than Zn. Only a small fraction of Cd condenses into pyroxene. Troilite, condensing at lower  $T$  than enstatite, serves as the major host for Cd.

### 3.3.5. Lithophile Elements Condensing in Feldspar: B, Cs, Ga, K, Na, and Rb

Feldspar, the solid solution series of anorthite, albite, and orthoclase, is the primary host among meteoritic minerals for Na, K, Rb, Cs, B, and, to some extent, Ga. Condensation of feldspar begins with anorthite formation at 1387 K, and 50% of K and Na are condensed into solid solution



when temperatures have dropped by about 400 and 440 K, respectively. Previously, the condensation temperatures of the heavy alkali elements Rb and Cs were uncertain or unknown, mainly because the thermodynamic properties for Rb and Cs analogs to albite or orthoclase are not available. The condensation of Rb and Cs is modeled by assuming that Rb and Cs follow K in chemistry and that Rb and Cs silicates exchange with the analogous K silicate in the  $\text{KAlSi}_3\text{O}_8$  structure. Using these assumptions, the 50% condensation temperatures of Rb and Cs are 800 and 799 K, respectively, for a solar system composition gas.

Boron substitutes for Al in the feldspar lattice (see Lauretta & Lodders 1997), and is 50% condensed in feldspar at 908 K, which makes B somewhat less volatile than Na. Ga, like B, substitutes for Al, but Ga is also siderophile and condenses into both feldspar and Fe metal. The volatility of Ga excludes 50% condensation into Fe metal before feldspar becomes stable, leading to a Ga 50% condensation temperature which considers distribution of Ga between these two host phases.

### 3.3.6. *Siderophile Elements Condensing Into the Fe Alloy: Ag, As, Au, Bi, Co, Cr, Cu, Ge, Ni, P, Pb, Pd, Sb, Sn, and Te*

Pure iron metal would begin to condense at 1357 K, but condensation of iron already takes place when the refractory metal alloy forms. However, iron is much more abundant than all refractory metals taken together, and the refractory metal alloy composition becomes dominated by iron near the condensation temperature of pure iron. Therefore, it is more appropriate here to talk about trace metal condensation into solid solution with an iron alloy below 1357 K.

Metals with 50% condensation temperatures above 1300 K include Co, Ni, and Pd. The 50% condensation temperatures of more volatile P and Cr are in the 1200–1300 K range. Phosphorous condensation leads to formation of schreibersite ( $\text{Fe, Ni}_3\text{P}$ ), which is often associated with metal in meteorites. Allen & Mason (1973) and Mason & Graham (1970) find that the major hosts of Cr and P in meteorites are chromite ( $\text{FeCr}_2\text{O}_4$ ) and whitlockite [ $\text{Ca}_3(\text{PO}_4)_2$ ], which could appear at odds with Cr and P condensation into metal. However, formation of chromite and phosphate involves an oxidation process that takes place at lower temperatures than schreibersite formation and Cr condensation into the Fe alloy.

Cu, As, and Au enter the metal alloy to 50% between 1000–1100 K, and they are more volatile, siderophile elements. The elements Ag, Bi, Ge, Pb, Sb, Sn, and Te are the most volatile in this group, and their 50% condensation temperatures approach the appearance condensation temperature of FeS at 704 K.

### 3.3.7. *Chalcophile Elements Condensing into Troilite: Cd, Hg, In, Se, and Tl*

Troilite condensation starts at 704 K, when the Fe alloy is corroded by  $\text{H}_2\text{S}$  gas. However, the Fe abundance is about twice that of sulfur, and only half of all iron can be converted to FeS, leading to metal and sulfide coexisting at lower temperatures. Troilite is the host phase for condensation of Se, In, Tl, and Cd, which are typically found in chondritic troilite. Trace element sulfides, selenides, and tellurides are known to easily dissolve in FeS, and condensation of these species is assumed for many trace elements here

(Tables 8 and 9). Elements such as Te, Pb, and Ag may concentrate in meteoritic troilite, but they do not necessarily condense only into troilite. Many elements with strong chalcophile affinities are also siderophile, and if no sulfide is present, these elements can condense into metal first. Their 50% condensation temperatures into metal are then higher than the appearance condensation temperature of FeS. For example, a major fraction of Te and Pb first condenses into metal. Once troilite begins to form, the remaining Te and Pb is removed from the gas by preferential incorporation into troilite. In addition, some of the fraction of Te and Pb previously condensed into Fe alloy can be redistributed into troilite during the sulfurization of the Fe alloy because of a stronger affinity of Te and Pb to sulfide than to metal.

One important point is that the troilite condensation temperature is independent of total pressure (for total pressures  $<10^{-2}$  bar), whereas the condensation temperature of metal decreases with decreasing total pressure. This affects the host phase “selection” of the 50% condensation temperature. For example, at the chosen pressure of  $10^{-4}$  bar, Te and Pb are condensed by 50% into metal before troilite forms. At a lower pressure of  $10^{-6}$  bar, only ~3% of Te and Pb are condensed into metal before troilite forms, and troilite becomes their major condensation host. At  $10^{-6}$  bar, their 50% condensation temperatures are 694 K (Te) and 634 K (Pb).

One element condensing into troilite at a very low temperature (252 K) is mercury, which places it among the highly volatile elements (§ 3.4). The condensation temperature of Hg has been problematic for some time because the Hg abundance is very small (and uncertain; see § 2.3.6) and because metallic Hg has a very high vapor pressure. The calculation here assumes that formation of  $\text{HgS}$ ,  $\text{HgSe}$ , and  $\text{HgTe}$  in solid solution with FeS leads to Hg removal from the gas. The low condensation temperature of Hg is still above that of water ice (see below). The CI chondrites show aqueous alteration products, which means that water has accreted onto the meteorite parent body to some extent. One could then expect that Hg should be fully condensed and that CI chondrites should show the full solar system complement of Hg. The solar system abundance determination of Hg relies on theoretical neutron-capture element systematics (§ 2.3.6), and it would be of great interest to obtain reliable Hg analyses from uncontaminated CI chondrite samples to check whether or not Hg abundances in CI chondrites indeed reflect gas-solid equilibration to such low temperatures.

### 3.3.8. *Condensation of Halogens: F, Cl, Br, and I*

Halogen condensation temperatures are among the more uncertain ones, and previously there were no or only uncertain condensation temperatures available for I and Br. In meteorites, halogens are concentrated in fluor- and chlorine-apatite [ $\text{Ca}_5(\text{PO}_4)_3(\text{F, Cl})$ ], but Br and I have also been detected in troilite (Allen & Mason 1973; Mason & Graham 1970). Chlorine occurs in sodalite ( $\text{Na}_4[\text{Al}_3\text{Si}_3\text{O}_{12}]\text{Cl}$ ), which condenses before apatite. Sodalite can break down at lower temperatures during condensation or during metamorphic processes on meteorite parent bodies, so that Cl-bearing apatite may form.

Fluorine apatite condenses at 739 K, and its formation involves oxidation of schreibersite ( $\text{Fe}_3\text{P}$ ; § 3.3.6). In the absence of thermodynamic data for Br- and I-apatite, the Br

and I condensation is modeled by assuming substitutions of the Ca fluoride component in apatite by the respective Ca bromide and iodides. This leads to 50% condensation temperatures of  $\sim 546$  K (Br) and  $\sim 535$  K (I). Condensation of Br and I into FeS was considered, but the amount of FeBr<sub>2</sub> or FeI<sub>2</sub> dissolving into troilite was found to be negligible.

### 3.4. Highly Volatile Element Condensation: C, N, O, and Noble Gases

Condensation of C, N, and O at low temperatures produces the major fraction of solids, as the high-temperature condensates of all other elements (except the noble gases) only make up about one-third of all condensable material. However, the condensation temperatures and types of condensates of C and N (and to some extent of O) are affected by kinetic effects, which are considered in the next sections.

#### 3.4.1. Oxygen Condensation

Water ice condensation sets the benchmark temperature for the appearance of volatile ices. Some oxygen removal from the gas has already taken place with the formation of silicates and oxides. About 23% of all oxygen is bound to rocky elements (Al, Ca, Mg, Si, and Ti) before water ice condenses at 182 K. Magnetite formation from Fe metal at 371 K increases the amount of oxygen bound to rock to 26%. Magnetite formation decreases the condensation temperature of water ice by  $\sim 0.5$  K because then the water vapor partial pressure is lowered slightly. The formation of magnetite also has a small effect on the amount of water ice that condenses. However, it has been known for some time that magnetite formation via a gas-solid oxidation reaction is very slow. For example, complete oxidation of Fe metal in the solar nebula is not expected because the lifetime of the solar nebula is probably too short compared to reaction timescales of magnetite formation (e.g., Fegley 2000). Therefore, applications of the condensation temperature of magnetite must consider kinetic effects. On the other hand, magnetite formation is faster in an aqueous environment such as a meteorite parent body. Thus, the majority of magnetite observed in CI chondrites most likely originated from aqueous alteration and is not a condensate from nebular gas (see Hong & Fegley 1998 and references therein).

Slow reaction rates are also the reason that the formation of hydrated silicates is problematic at low temperatures and low total pressures (see, e.g., Fegley 1988, 2000; Fegley & Prinn 1989; Prinn & Fegley 1989). Here, hydrated silicates were not considered as sinks for oxygen condensation. If hydrated silicate condensation were to occur, such silicates would appear at temperatures between 200 and 300 K, which is in between the magnetite and water condensation temperatures. Similar to magnetite, the observed hydrated silicates in carbonaceous chondrites more likely formed on the meteorite parent bodies rather than directly from nebular gas because rock hydration at low temperatures and very low pressures is kinetically infeasible during the lifetime of the solar nebula (see Fegley 2000).

The condensation of water ice may also be influenced by the potential nonequilibrium chemistry of carbon. Changes in water condensation due to this effect are discussed in the following section.

#### 3.4.2. Carbon Condensation

Condensation of carbon-bearing compounds depends on the gas-phase equilibrium between CO and methane,



as a function of temperature. Under equilibrium conditions, carbon monoxide is the major carbon-bearing gas at high temperature, but is replaced by methane gas with decreasing temperature. At  $10^{-4}$  bar, this occurs below  $\sim 650$  K. Pure methane ice then condenses at 41 K. Another potential methane-bearing condensate is CH<sub>4</sub>·7H<sub>2</sub>O, but this clathrate hydrate requires more oxygen (i.e., a C/O ratio of 0.14) than is available (C/O = 0.5). The amount of water ice present can only bind about 9% of the total carbon in CH<sub>4</sub>·7H<sub>2</sub>O, which starts to condense at 78 K. Under equilibrium conditions the major fraction of carbon does not condense until the pure methane condensation temperature of 41 K is reached.

On the other hand, it has been known for quite some time that the carbon monoxide to methane reaction is very slow at low total pressures and temperatures (e.g., Lewis & Prinn 1980). If methane formation (and that of other hydrocarbons) is kinetically inhibited, two other cases of carbon condensation chemistry are viable. These cases are end-member cases, as is the equilibrium case described above, which should be kept in mind in applying condensation temperatures to a given low-temperature environment. Table 10 summarizes the condensation temperatures for the equilibrium case and the two nonequilibrium cases described next.

If hydrocarbon formation is kinetically inhibited, reaction (16) is replaced by the reaction



The thermodynamic activity of graphite, the reference state of carbon, increases with decreasing temperature and eventually surpasses unity. Instead of abundant methane gas formation (beginning below  $\sim 650$  K in the equilibrium case), graphite precipitation sets in at 626 K. The CO and CO<sub>2</sub> gas abundances then drop with decreasing temperature. Reaction (17) does not involve water, and the water ice condensation temperature remains at 182 K, as in the equilibrium case above.

TABLE 10  
CONDENSATION TEMPERATURES (K) OF ICES

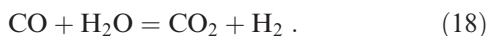
Compound	Complete Equilibrium	Kinetic Model A <sup>a</sup>	Kinetic Model B <sup>b</sup>
H <sub>2</sub> O .....	182	182	182–121
CH <sub>4</sub> ·7H <sub>2</sub> O .....	78	...	...
CH <sub>4</sub> .....	41	...	...
Graphite .....	...	626	<626
NH <sub>3</sub> ·H <sub>2</sub> O .....	131	...	...
N <sub>2</sub> ·7H <sub>2</sub> O .....	...	58	58

NOTE.—At  $10^{-4}$  bar total pressure. Solar system composition gas. Ellipses indicates that a compound does not form.

<sup>a</sup> Model A: Hydrocarbon and H-N gas formation kinetically inhibited.

<sup>b</sup> Model B: Hydrocarbon and H-N gas formation kinetically inhibited and graphite precipitation suppressed.

The third case for carbon condensation considers kinetic inhibition of hydrocarbon formation and suppressed graphite precipitation. If hydrocarbons cannot form at all and graphite condensation is also kinetically inhibited to some extent, CO remains the stable gas because reactions (16) and (17) cannot proceed to the right. However, CO can react with water, and CO is replaced by CO<sub>2</sub> as the major carbon-bearing gas with decreasing temperature according to the reaction



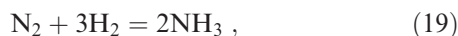
This reaction takes place below 650 K, starting at much higher temperatures than water ice condensation under equilibrium (§ 3.4.1), so water gas is present for CO<sub>2</sub> formation by reaction (18). With decreasing temperature, reaction (18) shifts to the right-hand side and the CO<sub>2</sub> gas abundance increases at the expense of CO and H<sub>2</sub>O gas. Because reaction (18) lowers the water vapor pressure, the condensation temperature of water ice drops to 121 K, much lower than the 182 K for equilibrium or the second case above. Condensation of water ice then fixes the water vapor pressure in reaction (18), and CO<sub>2</sub> and CO gas abundances drop as oxygen is depleted from the gas. Therefore, CO and CO<sub>2</sub> cannot reach their saturation vapor pressures and CO and CO<sub>2</sub> ices do not form.

As the removal of O into H<sub>2</sub>O ice depletes the gas of oxygen, the carbon oxides would be replaced by C- and N-bearing gases below 121 K. However, near the condensation temperature of water, the gas is extremely supersaturated in carbon, and even if hydrocarbon gas formation is prevented, graphite precipitation is expected. The condensation temperature of graphite then depends on the tolerable carbon supersaturation value, which already reaches about 700 times the equilibrium value at 500 K. Therefore, graphite precipitation is expected at some temperature below 626 K, where the graphite activity reaches unity (if hydrocarbon formation is inhibited). This means that the water condensation temperature for this case also depends on the temperature at which graphite precipitation sets in. The minimum water condensation temperature is in the range from 121 K (no graphite precipitation above 121 K) to 182 K (graphite precipitation at 626 K).

In neither case above is the formation of CO-bearing ices expected, because CO is converted to CH<sub>4</sub> (g), graphite, or CO<sub>2</sub>. This may not rule out the possibility that CO ices may form when other kinetic pathways are considered. However, this is beyond the scope of this paper.

### 3.4.3. Nitrogen Condensation

Nitrogen condensation chemistry is tied to the gas equilibrium



favoring ammonia gas formation at low temperatures (and high pressures). At 10<sup>-4</sup> bar, ammonia is the major N-bearing gas below ~325 K. As for carbon above, kinetics determine whether or not reaction (19) proceeds to equilibrium (Lewis & Prinn 1980), and two cases for nitrogen condensation are considered here. Under equilibrium conditions, ammonia hydrate (NH<sub>3</sub>·H<sub>2</sub>O) condenses at 131 K by the reaction of ammonia gas and water ice, and 50% of all nitrogen is in this hydrate by 123 K.

The kinetic inhibition of molecular nitrogen to ammonia gas formation or to any other N-H-bearing compounds is the other end-member case for nitrogen condensation. If molecular nitrogen remains the major N-bearing gas, N<sub>2</sub> is the expected constituent of N-bearing condensates such as N<sub>2</sub>·7H<sub>2</sub>O, N<sub>2</sub>·6 H<sub>2</sub>O, or N<sub>2</sub> ice. The formation of N<sub>2</sub> clathrate hydrate depends on the availability of water ice. The amount of water ice is not sufficient to bind all N<sub>2</sub> to N<sub>2</sub>·7H<sub>2</sub>O, but just about right for N<sub>2</sub>·6H<sub>2</sub>O. Condensation begins with N<sub>2</sub>·7H<sub>2</sub>O (s) at 58 K, which takes only a small fraction of total nitrogen. Subsequently, nitrogen condenses as N<sub>2</sub>·6H<sub>2</sub>O, and 50% of nitrogen is condensed by 52 K. This assumes that no water ice is consumed by methane clathrate, which is reasonable because if the N<sub>2</sub> to ammonia conversion is kinetically inhibited, so should be the CO to CH<sub>4</sub> conversion, and methane clathrate would not form. However, the N<sub>2</sub> clathrate hydrate condensation temperature is below the water ice condensation temperature irrespective of whether or not graphite condensation is taking place (§ 3.3.2).

### 3.3.4. Noble Gas Condensation

Among the noble gases, only the heavier ones are likely to condense. Helium partial pressures are much too small to reach the vapor pressure over liquid He, and temperatures below the space background temperature of ~3 K would be required for He to condense. The condensation temperature of 9 K for solid Ne is also fairly low. The noble gases Ar, Kr, and Xe can form clathrate hydrates of the form X·6H<sub>2</sub>O, and only a relatively small fraction (~0.04) of the total water ice is needed for clathrate hydrate formation. The condensation temperatures of the clathrate hydrates of Ar, Kr, and Xe are at 48, 53, and 69 K, respectively.

## 4. CONCLUSIONS

The heavy-element fractionation processes in the Sun make it necessary to distinguish two elemental abundance sets: the photospheric, fractionated abundances and the solar system, unfractionated abundances. Meteoritic abundances from CI chondrites are only suitable to refine the relative abundances of the heavy elements but cannot be used to constrain the absolute element/hydrogen ratios or the total mass fractions X, Y, and Z. When elemental abundances are normalized to the cosmochemical scale of Si = 10<sup>6</sup> atoms, only the H and He abundances are different for both abundance sets. The solar photosphere has a lower metallicity of about 84% of that of the proto-Sun. The difference in metallicity causes higher condensation temperatures (by ~10 K) for the gas of solar system composition.

The 50% condensation temperatures give the volatility groupings for the elements with solar system abundances at 10<sup>-4</sup> bar, as follows. *Ultrarefractory* elements with 50% condensation temperatures above 1650 K are the metals Os, Re, and W, the lithophile elements Al, Hf, Sc, Th, Y, Zr, and the heavy rare earth elements Gd, Tb, Dy, Ho, Er, Tm, and Lu. *Highly refractory* elements with 50% condensation temperatures between 1650 and 1500 K are the metals Ir, Mo, and Ru, and the lithophile elements Ca, Nb, Ta, Ti, U, and the light REE La, Pr, Nd, and Sm. *Refractory* elements have 50% condensation temperatures between 1500 and 1360 K. They include the metals Pt and Rh, and the lithophile elements Ba, Be, Ce, Sr, V, and Yb. The condensation



TABLE 11  
CONDENSATE DISTRIBUTION

Condensate	Solar System Composition	Solar Photospheric Composition	Literature Solar Composition <sup>a</sup>
Silicates and oxides .....	0.303	0.269	0.264
Metal + FeS.....	0.186	0.165	0.176
Total rock .....	0.489	0.434	0.440
H <sub>2</sub> O ice .....	0.571	0.506	0.920
CH <sub>4</sub> ice.....	0.330	0.292	0.408
NH <sub>3</sub> ice .....	0.097	0.086	0.134
Total ices.....	0.998	0.884	1.462
Total condensates.....	1.487	1.318	1.903
Rock among condensates.....	32.89	32.89	23.14
Ices among condensates .....	67.11	67.11	76.84
H <sub>2</sub> O ice/rock .....	1.17	1.17	2.09
Total oxygen in rock.....	22.75	22.75	14.42

NOTE.—Mass percent, assuming equilibrium condensation and excluding noble gas condensates.

<sup>a</sup> Anders & Grevesse 1989.

temperature range of 1360–1290 K of the *common elements* Mg, Si, and Fe is shared by the metals Co, Cr, Ni, and Pd, and lithophile Eu. The *moderately volatile* elements have 50% condensation temperatures between 1290 and 704 K, before FeS appears. This group contains the siderophile elements Ag, As, Au, Bi, Cu, Ga, Ge, P, Pb, Sb, and Te, the lithophile elements Cs, B, K, Li, Na, Mn, Rb, and Zn, and the halogens Cl and F. Troilite condensation marks the high end of the temperature range for *volatile* element condensation between 704 and 371 K, where 50% condensation of the chalcophile elements Cd, In, S, Se, and Tl occurs. The siderophile Sn and the halogens Br and I also belong to the volatile elements. The *highly volatile* elements C, N, O, noble gases, and Hg condense (if at all) below 371 K.

The recent downward revisions for C, N, and O abundances introduce significant changes in the mass of total condensate expected from both the photospheric and solar-composition abundance sets, when compared to the solar abundances from Anders & Grevesse (1989). Table 11 summarizes the condensate mass distribution between rocky and icy matter for the three elemental abundance sets. The largest amount of condensate is obtained for the solar composition by Anders & Grevesse (1989), where  $\sim 1.9\%$  of the

total mass ends up in condensate (the contribution in mass from noble gas condensates is excluded here). The solar system composition yields only 1.5% total condensate mass, the photospheric composition slightly less (1.3%). In all cases, the rocky matter makes up  $\sim 0.44\%$  to 0.49% of the total mass, and most of the condensed mass is from low-temperature ices. The Anders & Grevesse (1989) composition yields a water/ice to rock ratio of  $\sim 2$ , which is reduced to about unity for the solar system and photospheric compositions. These changes are important for modeling the chemistry of the outer solar nebula and for models of the formation of the giant planets and their satellites and of comets.

I thank Herbert Palme for a detailed referee report and useful suggestions. I also thank Al Cameron for his comments that improved the noble gas abundance data and their discussion. Many thanks to Roberto Gallino for drawing my attention to the recent Xe cross section measurements. I especially thank Bruce Fegley for much critical and patient advice on the various topics. Helpful comments by Laura Schaefer on the manuscript were also welcome. Work supported by NAG5-10553.

#### REFERENCES

- Allen, R., & Mason, B. 1973, *Geochim. Cosmochim. Acta*, 37, 1435  
 Allende Prieto, C., Lambert, D. L., & Asplund, M. 2001, *ApJ*, 556, L63  
 ———. 2002, *ApJ*, 573, L137  
 Anders, E., & Ebihara, M. 1982, *Geochim. Cosmochim. Acta*, 46, 2363  
 Anders, E., & Grevesse, N. 1989, *Geochim. Cosmochim. Acta*, 53, 197  
 Andersen, T., Petersen, P., & Hauge, O. 1976, *Sol. Phys.*, 49, 211  
 Balachandran, S. C., & Bell, R. A. 1998, *Nature*, 392, 791  
 Barklem, P. S., & O'Mara, B. J. 2000, *MNRAS*, 311, 535  
 Baumüller, D., Butler, K., & Gehren, T. 1998, *A&A*, 338, 637  
 Bergström, H., Biéumont, E., Lundberg, H., & Persson, A. 1988, *A&A*, 192, 335  
 Berzonsh, U., Svanberg, S., & Biéumont, E. 1997, *A&A*, 326, 412  
 Biéumont, E., Garnier, H. P., Pameri, P., Li, Z. S., & Svanberg, S. 2000, *MNRAS*, 312, 116  
 Biéumont, E., Grevesse, N., Faires, L. M., Marsden, G., & Lawler, J. E. 1989, *A&A*, 209, 391  
 Biéumont, E., Grevesse, N., Hannaford, P., Lowe, R. M., & Whaling, W. 1983, *ApJ*, 275, 889  
 Biéumont, E., Grevesse, N., & Hauge, O. 1979, *Sol. Phys.*, 61, 17  
 Biéumont, E., Grevesse, N., & Huber, M. C. E. 1978, *A&A*, 67, 87  
 Biéumont, E., Grevesse, N., Huber, M. C. E., & Sandeman, R. J. 1980, *A&A*, 87, 242  
 Biéumont, E., Grevesse, N., Kwiatkowski, M., & Zimmermann, P. 1984, *A&A*, 131, 364  
 Biéumont, E., Lynga, C., Li, Z. S., Svanberg, S., Garnier, H. P., & Doidge, P. S. 1999, *MNRAS*, 303, 721  
 Biéumont, E., Martin, F., Quinet, P., & Zeippen, C. J. 1994, *A&A*, 283, 339  
 Biéumont, E., Quinet, P., & Zeippen, C. J. 1993, *A&AS*, 102, 435  
 Biéumont, E., & Youssef, N. Y. 1984, *A&A*, 140, 177  
 Bizzarri, A., Huber, M. C. E., Noels, A., Grevesse, N., Bergeson, S. D., Tsekiris, P., & Lawler, J. E. 1993, *A&A*, 273, 707  
 Bizarro, M., Baker, J. A., Haack, H., Ulfbeck, D., & Rosing, M. 2003, *Nature*, 421, 931  
 Boesgaard, A. M., Deliyannis, C. P., King, J. R., & Stephens, A. 2001, *ApJ*, 553, 754  
 Booth, A. J., Blackwell, D. E., & Shallis, M. J. 1984, *MNRAS*, 209, 77  
 Boothroyd, A. I., & Sackmann, I. J. 2003, *ApJ*, 583, 1004  
 Bord, D. J., & Cowley, C. R. 2002, *Sol. Phys.*, 211, 3  
 Bord, D. J., Cowley, C. R., & Mirijanian, D. 1998, *Sol. Phys.*, 178, 221  
 Boynton, W. V. 1975, *Geochim. Cosmochim. Acta*, 39, 569  
 Cameron, A. G. W. 1973, *Space Sci. Rev.*, 15, 121  
 ———. 1982, in *Essays in Nuclear Astrophysics*, ed. C. A. Barnes, D. D. Clayton, & D. N. Schramm (Cambridge: Cambridge Univ. Press), 23  
 Cardon, B. L., Smith, P. L., Scalo, J. M., & Testerman, I. 1982, *ApJ*, 260, 395  
 Carlsson, M., Rutten, R. J., Brules, J. H. M. J., & Shchukina, N. G. 1994, *A&A*, 288, 860

- Case, D. R., Laul, L. C., Pelly, I. Z., Wechter, M. A., Schmidt-Bleek, F., & Lipschutz, M. E. 1973, *Geochim. Cosmochim. Acta*, 37, 19
- Chase, M. W. 1999, NIST-JANAF Thermochemical Tables (4th Ed.; J. Phys. Chem. Ref. Data Monogr. 9)
- Chen, J. H., Papanastassiou, D. A., & Wasserburg, G. J. 1998, *Geochim. Cosmochim. Acta*, 49, 1681
- Chen, Y. Q., Nissen, P. E., Zhao, G., & Asplund, M. 2002, *A&A*, 390, 225
- Chiemlewski, Y., Müller, E. A., & Braut, J. M. 1975, *A&A*, 42, 37
- Christensen-Dalsgaard, J. 1998, *Space Sci. Rev.*, 85, 19
- . 2002, *Rev. Mod. Phys.*, 74, 1073
- Cunha, K., & Smith, V. V. 1999, *ApJ*, 512, 1006
- Curtis, D. B., & Gladney, E. S. 1985, *Earth Planet. Sci. Lett.*, 75, 311
- Del Zanna, G., Bromage, B. J. I., & Mason, H. E. 2003, *A&A*, 398, 743
- Dreibus, G., Palme, H., Spettel, B., Zipfel, J., & Wänke, H. 1995, *Meteoritics*, 30, 439
- Dziembowski, W. A. 1998, *Space Sci. Rev.*, 85, 37
- Ebel, D. S., & Grossman, L. 2000, *Geochim. Cosmochim. Acta*, 64, 339
- Eisentraut, K. J., Griest, D. J., & Sievers, R. E. 1971, *Anal. Chem.*, 43, 2003
- Fegley, B. 1988, In *Workshop on the Origins of Solar Systems*, ed. J. A. Nuth & P. Sylvester (Houston: LPI Tech. Rep. 88-04), 51
- . 2000, *Space Sci. Rev.*, 92, 177
- Fegley, B., & Lewis, J. S. 1980, *Icarus*, 41, 439
- Fegley, B., & Lodders, K. 1994, *Icarus*, 110, 117
- Fegley, B., & Palme, H. 1985, *Earth Planet. Sci. Lett.*, 72, 311
- Fegley, B., & Prinn, R. G. 1989, in *The Formation and Evolution of Planetary Systems*, ed. H. Weaver & L. Danly (Cambridge: Cambridge Univ. Press), 171
- Folinsbee, R. E., Douglas, J. A. V., & Maxwell, J. A. 1967, *Geochim. Cosmochim. Acta*, 31, 1625
- Fredriksson, K., & Kerridge, J. F. 1988, *Meteoritics*, 23, 35
- Gabriel, M. 1997, *A&A*, 327, 771
- Göpel, C., Manhès, G., & Allègre, C. J. 1985, *Geochim. Cosmochim. Acta*, 62, 3379
- Gratton, R. G., & Sneden, C. 1994, *A&A*, 287, 927
- Grevesse, N. 1984, *Phys. Scr.*, 8, 49
- Grevesse, N., Blackwell, D. E., & Petford, A. D. 1989, *A&A*, 208, 157
- Grevesse, N., & Noels, A. 1993, in *Origin and Evolution of the Elements*, ed. N. Prantzos, E. Vangioni-Flam, & M. Cassé (Cambridge: Cambridge Univ. Press), 15
- Grevesse, N., Noels, A., & Sauval, A. J. 1993, *A&A*, 271, 587
- . 1996, in *ASP Conf. Ser. 99, Cosmic Abundances*, ed. S. S. Holt & G. Sonneborn (San Francisco: ASP), 117
- Grevesse, N., & Sauval, A. J. 1998, *Space Sci. Rev.*, 85, 161
- . 2002, *Adv. Space Res.*, 30, 3
- Grossman, L. 1972, *Geochim. Cosmochim. Acta*, 36, 597
- Grossman, L., & Larimer, J. W. 1974, *Rev. Geophys. Space Phys.*, 12, 71
- Gurvich, L. V., Veyts, I. V., & Alcock, C. B. 1989, *Thermodynamic Properties of Individual Substances* (New York: Hemisphere)
- Hall, D. N. B., & Noyes, R. W. 1969, *ApJ*, 4, L143
- . 1972, *ApJ*, 175, L95
- Hannaford, P., Lowe, R. M., Biéumont, E., & Grevesse, N. 1985, *A&A*, 143, 447
- Hauge, Ö. 1972, *Sol. Phys.*, 26, 263
- Holweger, H. 2001, in *AIP Conf. Proc. 598, Solar and Galactic Composition: A Joint SOHO/ACE Workshop*, ed. R. F. Wimmer-Schweingruber (New York: AIP), 23
- Holweger, H., & Werner, K. 1982, *Sol. Phys.*, 81, 3
- Hong, Y., & Fegley, B. 1998, *Meteor. Planet. Sci.*, 33, 1101
- Jacobsen, S. B., & Wasserburg, G. J. 1984, *Earth Planet. Sci. Lett.*, 67, 137
- Kiselman, D., & Carlsson, M. 1996, *A&A*, 311, 680
- Kohl, J. L., Parkinson, W. H., & Withbroe, G. L. 1977, *ApJ*, 212, L101
- Kornacki, A. S., & Fegley, B. 1986, *Earth Planet. Sci. Lett.*, 79, 217
- Krot, A. N., Fegley, B., Palme, H., & Lodders, K. 2000, in *Protostars and Planets IV*, ed. V. Mannings, A. P. Boss, & S. S. Russell (Tucson: Univ. of Arizona Press), 1019
- Kwiatkowski, M., Zimmermann, P., Biéumont, E., & Grevesse, N. 1982, *A&A*, 112, 337
- . 1984, *A&A*, 135, 59
- Lambert, D. L., & Luck, R. E. 1978, *MNRAS*, 183, 79
- Lambert, D. L., Mallia, E. A., & Smith, G. 1972, *Sol. Phys.*, 26, 250
- Lambert, D. L., Mallia, E. A., & Warner, B. 1969, *MNRAS*, 142, 71
- Larimer, J. W. 1967, *Geochim. Cosmochim. Acta*, 31, 1215
- . 1973, *Geochim. Cosmochim. Acta*, 37, 1603
- . 1975, *Geochim. Cosmochim. Acta*, 39, 389
- . 1988, in *Meteorites and the Early Solar System*, ed. J. F. Kerridge & M. S. Matthews (Tucson: Univ. Arizona Press), 345
- Larimer, J. W., & Bartholomay, M. 1979, *Geochim. Cosmochim. Acta*, 43, 1455
- Lauretta, D. S., & Lodders, K. 1997, *Earth Planet. Sci. Lett.*, 146, 315
- Lawler, J. E., Bonvallet, G., & Sneden, C. 2001, *ApJ*, 556, 452
- Lawler, J. E., Wickliffe, M. E., Cowley, C. R., & Sneden, C. 2001a, *ApJS*, 137, 314
- Lawler, J. E., Wickliffe, M. E., Den Hartog, E. A., & Sneden, C. 2001b, *ApJ*, 563, 1075
- Lewis, G. N., & Randall, M. 1961, *Thermodynamics* (2d ed; New York: McGraw Hill)
- Lewis, J. S., & Prinn, R. G. 1980, *ApJ*, 238, 357
- Liumbimkov, L. S., & Zalaetdinova, N. G. 1987, *Krymskaia Astrofiz. Obs. Isvest.*, 76, 102
- Lodders, K. 1999, *J. Phys. Chem. Ref. Data*, 28, 1705
- . 2003, *J. Phys. Chem. Ref. Data*, in press
- Lodders, K., & Fegley, B. 1993, *Earth Planet. Sci. Lett.*, 117, 125
- . 1995, *Meteoritics*, 30, 661
- . 1997, *AIP Conf. Proc. 402, Astrophysical Implications of the Laboratory Study of Presolar Materials*, ed. T. J. Bernatowicz & E. Zinner (New York: AIP), 391
- Lodders, K., & Fegley, B. 1998, *The Planetary Scientist's Companion* (New York: Oxford Univ. Press)
- Lord, H. C. 1965, *Icarus*, 4, 279
- Mason, B. 1963, *Space Sci. Rev.*, 1, 621
- Mason, B., & Graham, A. L. 1970, *Smithsonian Contrib. Earth Sci.*, 3, 1
- Meyer, J. P. 1989, in *AIP Conf. Proc. 183, Cosmic Abundances of Matter*, ed. C. J. Waddington (New York: AIP), 240
- . 1996, in *ASP Conf. Ser. 99, Cosmic Abundances*, ed. S. S. Holt & G. Sonneborn (San Francisco: ASP), 127
- Minster, J. F., Birck, J. L., & Allègre, C. J. 1982, *Nature*, 300, 414
- Neuforge, C. 1993, in *Origin and Evolution of the Elements*, ed. N. Prantzos, E. Vangioni-Flam, & M. Cassé (Cambridge: Cambridge Univ. Press), 63
- Palme, H., & Beer, H. 1993, in *Landolt Börnstein Group VI, Astronomy and Astrophysics*, Vol. 2A, ed. H. H. Voigt (Berlin: Springer), 196
- Palme, H., & Fegley, B. 1990, *Earth Planet. Sci. Lett.*, 101, 180
- Prinn, R. G., & Fegley, B. 1989, in *Origin and Evolution of Planetary and Satellite Atmospheres*, ed. S. Atreya, J. Pollack, & M. S. Matthews (Tucson: Univ. Arizona Press), 78
- Quandt, U., & Herr, W. 1974, *Earth Planet. Sci. Lett.*, 24, 53
- Raiteri, C. M., Gallino, R., Busso, M., Neuberger, D., & Käppeler F. 1993, *ApJ*, 419, 207
- Reames, D. V. 1998, *Space Sci. Rev.*, 85, 327
- Reed, G. W., & Jovanovic, S. 1967, *J. Geophys. Res.*, 72, 2219
- Reifarth, R., Heil, M., Käppeler, F., Voss, F., & Wisshak, K. 2002, *Phys. Rev. C*, 66, 064603
- Richard, O., Dziembowski, W. A., Seinkiewicz, R., & Goode, P. R. 1998, *A&A*, 338, 756
- Rosman, K. J. R., & Taylor, P. D. P. 1998, *J. Phys. Chem. Ref. Data*, 27, 1275
- Ross, J. E., & Aller, L. H. 1976, *Science*, 191, 1223
- Russell, H. N. 1934, *ApJ*, 79, 317
- Saxena, S. K., & Eriksson, G. 1983, *Earth Planet. Sci. Lett.*, 65, 7
- Sears, D. W. 1978, *Earth Planet. Sci. Lett.*, 41, 128
- Sill, C. W., & Willis, C. P. 1962, *Geochim. Cosmochim. Acta*, 26, 1209
- Sneden, C., & Crocker, D. A. 1988, *ApJ*, 335, 406
- Spettel, B., Palme, H., Dreibus, G., & Wänke, H. 1994, *Meteoritics*, 28, 440
- Suess, H. E., & Urey, H. C. 1956, *Rev. Mod. Phys.*, 28, 53
- Takada-Hidai, M., Takeda, Y., Sato, S., Honda, S., Sadakane, K., Kawanomoto, S., Sargent, W. L., Lu, L., & Barlow, T. A. 2002, *ApJ*, 573, 614
- Vilesek, E. 1977, *Meteoritics*, 12, 373
- Wai, C. M., & Wasson, J. T. 1977, *Earth Planet. Sci. Lett.*, 36, 1
- . 1979, *Nature*, 282, 790
- Walker, R. J., Morgan, J. W., Beary, E. S., Smoliar, M. I., Czamanske, G. K., & Horan, M. F. 1997, *Geochim. Cosmochim. Acta*, 61, 4799
- Walter, G., & Beer, H. 1983, *A&A*, 123, 279
- Ward, L., Vogel, O., Arnesen, A., Hallin, P., & Wännström, A. 1985, *Phys. Scr.*, 31, 161
- Wasson, J. T. 1985, *Meteorites* (Berlin: Springer), 267
- Widing, K. G. 1997, *ApJ*, 480, 400
- Wieler, R. 2002, in *Noble Gases in Geochemistry and Cosmochemistry*, ed. D. Porcelli, C. J. Ballentine, & R. Wieler (Washington: Geochemical Soc. America), 21
- Wildt, R. 1933, *Z. Astrophys.*, 6, 345
- Wolf, D., & Palme, H. 2001, *Meteor. Planet. Sci.*, 36, 559
- Young, P. R., Mason, H. E., Keenan, F. P., & Widing, K. G. 1997, *A&A*, 323, 243
- Youssef, N. H., & Amer, M. A. 1989, *A&A*, 220, 281
- Youssef, N. H., Dönszelmann, A., & Grevesse, N. 1990, *A&A*, 239, 367
- Youssef, N. H., & Khalil, N. M. 1987, *A&A*, 186, 333
- . 1988, *A&A*, 203, 378
- Zhai, M., & Shaw, D. 1994, *Meteoritics*, 29, 607